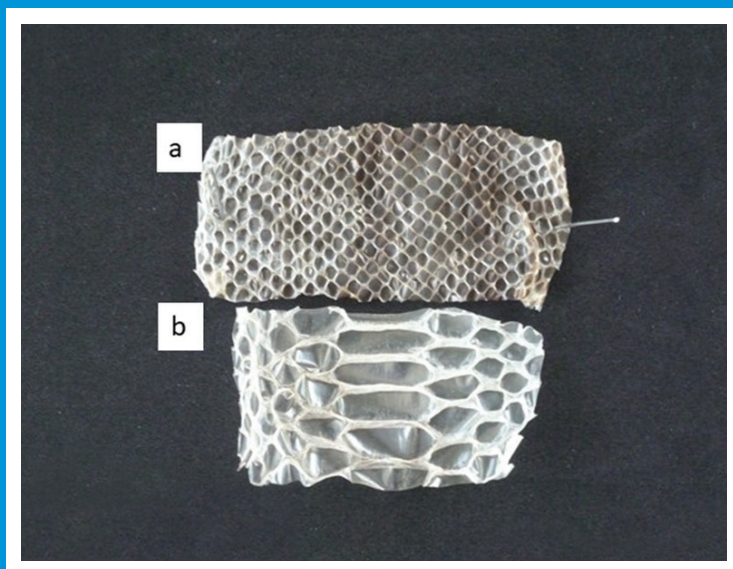


THE SCIENTIFIC JOURNAL OF THE VETERINARY FACULTY UNIVERSITY OF LJUBLJANA

SLOVENIAN VETERINARY RESEARCH

SLOVENSKI VETERINARSKI ZBORNIK



Volume
57 2

THE SCIENTIFIC JOURNAL OF THE VETERINARY FACULTY UNIVERSITY OF LJUBLJANA

SLOVENIAN VETERINARY RESEARCH

SLOVENSKI VETERINARSKI ZBORNIK

Volume
57 2

Slov Vet Res • Ljubljana • 2020 • Volume 57 • Number 2 • 45–100

The Scientific Journal of the Veterinary Faculty University of Ljubljana

SLOVENIAN VETERINARY RESEARCH
SLOVENSKI VETERINARSKI ZBORNIK

Previously: RESEARCH REPORTS OF THE VETERINARY FACULTY UNIVERSITY OF LJUBLJANA
Prej: ZBORNIK VETERINARSKE FAKULTETE UNIVERZA V LJUBLJANI

4 issues per year / izhaja štirikrat letno

Editor in Chief / glavni in odgovorni urednik: Gregor Majdič

Co-Editor / sourednik: Modest Vengušt

Technical Editor / tehnični urednik: Matjaž Uršič

Assistants to Editor / pomočnici urednika: Valentina Kubale Dvojmoč, Klementina Fon Tacer

Editorial Board / uredniški odbor:

Vesna Cerkvenik, Robert Frangež, Polona Juntos, Tina Kotnik, Uroš Krapež, Matjaž Ocepek, Joško Račnik, Ivan Toplak, Milka Vrecl,
Veterinary Faculty University of Ljubljana / Veterinarska fakulteta Univerze v Ljubljani

Editorial Advisers / svetovalca uredniškega odbora: Gita Greco-Smole for Bibliography (bibliotekarka),

Leon Ščuka for Statistics (za statistiko)

Reviewing Editorial Board / ocenjevalni uredniški odbor:

Antonio Cruz, Paton and Martin Veterinary Services, Adegrove, British Columbia; Gerry M. Dorrestein, Dutch Research Institute for Birds and Exotic Animals, Veldhoven, The Netherlands; Sara Galac, Utrecht University, The Netherlands; Wolfgang Henninger, Veterinärmedizinische Universität Wien, Austria; Simon Horvat, Biotehniška fakulteta, Univerza v Ljubljani, Slovenia; Nevenka Kožuh Eržen, Krka, d.d., Novo mesto, Slovenia; Louis Lefaucheur, INRA, Rennes, France; Peter O'Shaughnessy, Institute of Comparative Medicine, Faculty of Veterinary Medicine, University of Glasgow, Scotland, UK; Peter Popelka, University of Veterinary Medicine, Košice, Slovakia; Detlef Rath, Institut für Tierzucht, Forschungsbericht Biotechnologie, Bundesforschungsanstalt für Landwirtschaft (FAL), Neustadt, Germany; Henry Stämpfli, Large Animal Medicine, Department of Clinical Studies, Ontario Veterinary College, Guelph, Ontario, Canada; Frank J. M. Verstraete, University of California Davis, Davis, California, US; Thomas Wittek, Veterinärmedizinische Universität, Wien, Austria

Address: Veterinary Faculty, Gerbičeva 60, 1000 Ljubljana, Slovenia

Naslov: Veterinarska fakulteta, Gerbičeva 60, 1000 Ljubljana, Slovenija

Tel.: +386 (0)1 47 79 100, Fax: +386 (0)1 28 32 243

E-mail: slovetres@vf.uni-lj.si

Sponsored by the Slovenian Research Agency

Sofinancira: Javna agencija za raziskovalno dejavnost Republike Slovenije

ISSN 1580-4003

Printed by/tisk: DZS, d.d., Ljubljana, June 2020

Indexed in/indeksirano v: Agris, Biomedicina Slovenica, CAB Abstracts, IVSI

Ulrich's International Periodicals Directory, Science Citation Index Expanded,

Journal Citation Reports – Science Edition

<http://www.slovetres.si/>

SLOVENIAN VETERINARY RESEARCH SLOVENSKI VETERINARSKI ZBORNIK

Slov Vet Res 2020; 57 (2)

Original Research Articles

Skoczylas B, Brudnicki W, KirkiŃo-Stacewicz K, Nowicki W, Wach J. Cortical branches of the middle cerebral artery in European badger (<i>Meles meles</i>)	49
Tozon N, Biasizzo M, Šćuka L, Potoćnik T, Redek M, Prem L. Reducing the number of bacterial colonies using Ecocid® S (potassium peroxy sulphate based disinfectant) at small animal clinic	55
Siddique AB, Rahman SU, Ulhaq M, Naveed R. Occurrence, molecular identification and antibiotic resistance profiling of <i>Mycoplasma gallisepticum</i> and <i>Mycoplasma synoviae</i> from chronic respiratory disease cases in poultry birds and farm environment	61
Sacha M, Weisbach N, Pöhler AS, Demmerle N, Haltner E. Comparisons of the histological morphology and <i>in vitro</i> percutaneous absorption of caffeine in shed snake skin and human skin	71
Aboubakr M, Elkomy A, Belih S, Morad M, Shaheen H, Abdel-Daim MM. Efficacy of amoxicillin (Atcomox®) and/or allicin on performance, haematological, biochemical, and histopathological changes in <i>Clostridium perfringens</i> infected chickens	83

CORTICAL BRANCHES OF THE MIDDLE CEREBRAL ARTERY IN EUROPEAN BADGER (*MELES MELES*)

Benedykt Skoczylas, Witold Brudnicki, Krzysztof Kirkiłło-Stacewicz*, Włodzimierz Nowicki, Jan Wach

UTP University of Science and Technology, Faculty of Animal Breeding and Biology, Department of Physiology, Zoophysiotherapy and Animal Breeding, Mazowiecka 28, 85-084 Bydgoszcz, Poland

*Corresponding author, E-mail: krzysztof.stacewicz@o2.pl

Abstract: The pattern and variation of the cortical branches of the middle cerebral artery in European badger were studied for 64 cerebral hemispheres. It was found that the artery bifurcates into splits into ten permanent branches. Two olfactory arteries supply the area of the brain situated on the border between the old and the new cortex. The other eight branches get divided into three branches heading for the frontal region, two branches – to the parietal region and three temporal branches which supply only the new cortex. The frontal, parietal and temporal branches descended independently from the main trunk of the middle cerebral artery or formed a common trunk first. Common trunks for respective groups of branches have been described as the rostral, dorsal and caudal middle cerebral artery. The rostral olfactory artery in 6.3% of the cases investigated was an independent branch from the rostral cerebral artery.

Key words: arteries; brain; European badger

Introduction

The first information on the anatomy of the middle cerebral artery in various mammals is given by Hofmann (1). In the applicable literature on the blood supply to the brain one can find papers discussing the pattern of descent of the middle cerebral artery and its division into cortical branches. The issues were described for domestic pig by Walinczus (2) who covered the range and the pattern of blood supply to respective cerebrum

regions. The pattern of the middle cerebral artery and its cortical branches in cat were described by Chadzypanagiotis (3); the author provides the nomenclature on respective cortical branches of that artery.

Systematic descriptions of the division and the pattern of the cortical branches of the middle cerebral artery in some Carnivora species are provided by Wiland (4), in wild boar – by Skoczylas & Wiland (5).

Over the recent years there have appeared numerous papers on the anatomy of the middle cerebral artery in various mammal species. The authors of those papers report on the respective

regions of the brain being supplied by the same arterial branches, which refers to the arteries which occur as single branches in grivet (6), in yellow baboon (7), in European otter (8) and multiple arteries in domestic pig (9).

The pattern of division of the middle cerebral artery is affected by various factors; e.g. the species represented and sulcus pattern of the cerebral cortex. In mammals on the surface of the cortex the sulcus pattern varies, which can affect the anatomy of the cortical branches of the middle cerebral artery (10). Considering the discrepancies resulting from respective descriptions and factoring in new research, it has been decided to investigate the pattern, the division and the variation in cortical branches of the middle cerebral artery in European badger and to compare the results with those reported by other authors.

Materials and methods

The studies of the middle cerebral artery involved 32 brains in European badger; in total 64 cerebral hemispheres obtained from hunting. Ethics approval was not required since animals died because of natural reasons. The research used the European badger heads cut off at the height of the 3rd -4th cervical vertebrae. The arteries were filled with latex introduced into common carotid artery with the medical syringe. This method was described by Godynicki (11). Having fixed the heads in 5% formalin solution

and having decalcified the skulls in hydrochloric acid, the skull cavity was opened and the brains were taken out. The cerebral hemispheres were photographed and their anatomy, division and pattern of the cortical branches of the middle cerebral artery were described.

Results

In European badger the blood is supplied to the brain with internal carotid arteries (Fig. 1a) and vertebral arteries.

The internal carotid artery, having entered the skull and perforated dura mater, bifurcates into the rostral cerebral artery (Fig. 1 b) and caudal communicating artery (Fig. 1c) which, together with the symmetrical vessels form the circle of Willis. From the initial section of the rostral cerebral artery, towards the cortex, there descends the middle cerebral artery.

The middle cerebral artery is the strongest vessel supplying blood to cerebrum. The initial section of the main trunk of the middle cerebral artery heads along the ventral surface of the optic tract and before the rostral border of piriform lobe. Then the section bends around the piriform lobe and goes through its rostral border. Further on it runs to the lateral rhinal sulcus and, having passed it, it gets divided. From the initial section of the main trunk of the middle cerebral artery there descend minor central branches supplying blood to olfactory tracts and the piriform lobe.

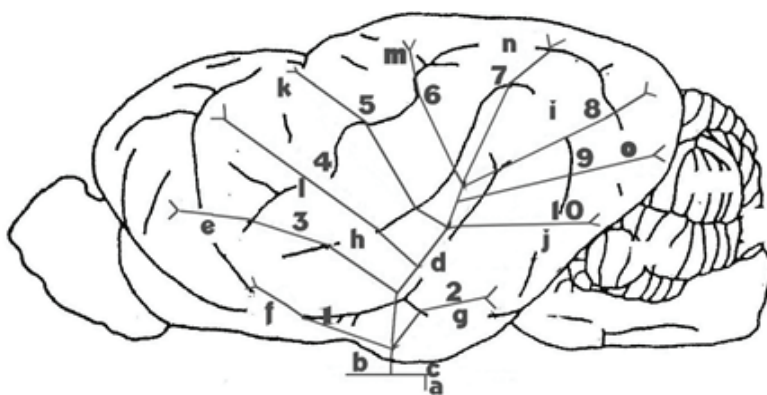


Figure 1: Pattern of division of the middle cerebral artery on the brain cortex in European badger.

1 – rostral olfactory artery, 2 – caudal olfactory artery, 3 – orbital branch, 4 – ventral frontal branch, 5 – dorsal frontal branch, 6 – rostral parietal branch, 7 – caudal parietal branch, 8 – dorsal temporal branch, 9 – middle temporal branch, 10 – ventral temporal branch, a – internal carotid artery, b – rostral cerebral artery, c – caudal communicating artery, d – Sylvian fissure, e – presylvian sulcus, f – rostral lateral rhinal sulcus, g – caudal lateral rhinal sulcus, h – rostral suprasylvian sulcus, i – middle suprasylvian sulcus, j – caudal suprasylvian sulcus, k – cruciate sulcus, l – coronary sulcus, m – ansiform sulcus, n – marginal sulcus, o – external marginal sulcus

The main trunk of the middle cerebral artery gets divided further into a number of cortical branches which head for the specific region of the cerebral hemisphere supplying blood to specific regions of the brain. The first permanent branches of the middle cerebral artery which supply blood to both the old and the new cortex are olfactory arteries.

The rostral olfactory artery (Fig. 2-1), having separated from the main trunk of the middle cerebral artery, goes towards the rostral part of the lateral rhinal sulcus it can ascend into in various places. Its terminal branches can also appear again from under the lateral rhinal sulcus and then disappear into the cortex located over that sulcus.

The caudal olfactory artery (Fig. 2 – 2) descends into the caudal part of the lateral rhinal sulcus. Its terminal branches supply blood to the area of the cortex found over that sulcus. The other arterial branches supply the regions of the cortex located over the lateral rhinal sulcus. On the cerebral cortex towards the frontal lobus there spread three thick branches.

The orbital branch (Fig. 2-3) descends first; it runs towards the region of the presylvian sulcus where its terminal branches reach the coronary groove.

The ventral frontal branch (Fig. 2-4) vascularises the middle parts of that region of the cortex. The branch of that vessel goes through the rostral suprasylvian sulcus towards the coronary sulcus.

The dorsal frontal branch (Fig.2-5), having separated from the middle cerebral artery goes up to the regions of the cruciate sulcus. Those vessels supply blood to the upper part of the medial surface of the frontal lobus. The successive vessel which runs towards the parietal lobus bifurcates into two branches.

The rostral parietal branch (Fig. 2-6) runs towards the ansiform sulcus. The terminal twigs of that vessel supply blood to the area of the cortex located behind the ansiform sulcus and run medially of the cerebral hemisphere.

The caudal parietal branch (Fig. 2-7) runs towards the region of the marginal sulcus and it branches out further into minor vessels; some of them ascend to the medial suprasylvian sulcus.

The lateral-caudal surface of the cerebral hemisphere is supplied by the branches of the middle cerebral arteries descending here one by one at various heights and they have been referred to as temporal branches.

The dorsal temporal branch (Fig. 2-8) is usually the most powerful cortical branch of the middle cerebral artery and its further prolongation in the area of the cortex. Having descended from the Sylvian fissure, it goes towards the external marginal sulcus. The branch supplies the upper part of the cortex.

The middle temporal branch (Fig. 2-9) descends a little distance from the previous branch. On the surface of the hemisphere it runs towards the caudal suprasylvian sulcus. Its terminal branches go onto the surface of the occipital lobus.

The ventral temporal branch (Fig. 2-10) goes to the end of the caudal suprasylvian sulcus. Having passed the caudal part of the sulcus, its terminal branches participate in supplying blood to a part of occipital lobus.

Considering the general pattern of the distribution of cortical branches of the middle cerebral artery in European badger presented here, one shall note that the respective sections of those branches can be found inside respective sulci, sometimes undergoing further divisions, always going towards of the cerebral cortex regions described.

Considering the pattern of descend of cortical branches of the middle cerebral artery in the European badger individuals studied, it was found that from the rostral cerebral artery on 60 cerebral hemispheres there descended one independent vessel; the middle cerebral artery. Among them on 15 (23.4%) hemispheres from the main trunk of the middle cerebral artery there descended rostrally a common trunk for the rostral olfactory artery and for the orbital branch, then a common descent for the ventral and dorsal frontal branches. The main trunk separated the caudal olfactory artery caudally with a common descent from the ventral temporal branch. Having descended into the Sylvian fissure, it brought a common trunk for rostral and caudal parietal branches as well as for the middle and dorsal temporal branches onto the surface of the cortex.

In another 11 (17.2%) cases from the main trunk of the middle cerebral artery there rostrally descended a common descent for rostral olfactory artery and for the orbital, ventral and dorsal frontal branches. Caudally from the main trunk there descended the caudal olfactory artery with a common trunk with ventral and middle temporal branches. The main trunk, having ascended to the Sylvian fissure brought a common descent for

parietal branches and the dorsal temporal branch onto the surface of the cortex

In yet another 9 (14.1%) cerebral hemispheres the rostral branch was made up by a common trunk for the rostral olfactory artery and the orbital, ventral and caudal frontal branches. The main trunk got onto the surface of the cortex from the Sylvian fissure and created a common descent for parietal branches. Caudally from the main trunk of the middle cerebral artery there separated, with a common trunk, the temporal branches with the caudal olfactory artery.

In 12 (18.7%) cases from the main trunk there rostrally descended an independent rostral olfactory artery, then a common descent for the orbital branch and for ventral and dorsal frontal branches. Caudally, from the main trunk there separated, with a common descent, the middle and ventral temporal branches as well as caudal olfactory artery. The main trunk, having ascended into the Sylvian fissure, brought a common trunk for rostral and caudal parietal branches as well as the dorsal temporal branch onto the surface of the cortex.

On another 13 (20.3%) hemispheres from the main trunk there rostrally separated the orbital

branch, the ventral frontal branch and the rostral olfactory artery with a common trunk. The main trunk of the middle cerebral artery, having appeared on the surface of the cortex, separated a common descent for the dorsal frontal branch as well as rostral and caudal parietal branches. Caudally from the main trunk there separated, with a common descent, ventral, middle and dorsal temporal branches and an independent caudal olfactory artery.

In the other 4 (6.3%) hemispheres it was found that from the rostral cerebral artery there descended two independent branches of the middle cerebral artery. The first independent branch from the rostral cerebral artery was the rostral olfactory artery, while the second branch from the rostral cerebral artery was the main trunk of the middle cerebral artery the orbital branch and frontal branches descended from rostrally with a common descent. The main trunk, having ascended to the Sylvian fissure, brought respectively, the rostral and caudal parietal branches as well as the dorsal temporal branch onto the cortex surface. Caudally from the main trunk there descended independent caudal olfactory artery, ventral and middle temporal branches (Fig. 2).

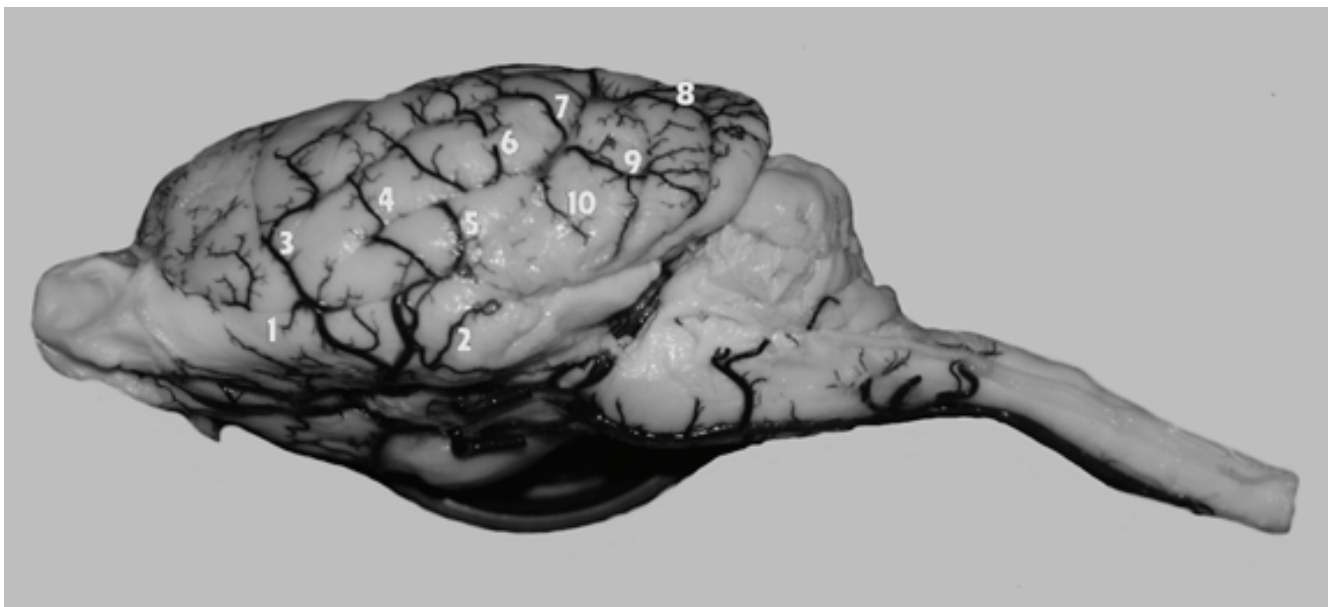


Figure 2: Lateral view of the independent descent of the rostral olfactory artery and the main trunk of the middle artery from the rostral cerebral artery

1 – Rostral olfactory artery, 2 – caudal olfactory artery, 3 – orbital branch, 4 – ventral frontal branch, 5 – dorsal frontal branch, 6 – rostral parietal branch, 7 – caudal parietal branch, 8 – dorsal temporal branch, 9 – middle temporal branch, 10 – ventral temporal branch

Discussion

In European badger the middle cerebral artery supplies blood to the same areas of the brain as in the mammal species investigated so far. The discrepancies concern mostly its division into respective branches. Chadzypanagiotis (3), describing the anatomy of the middle cerebral artery in cat, differentiated between the branches supplying the old cortex, the branches on the border of the old and the new cortex as well as the branches for the new cortex. In European badger the arteries supplying blood to the old cortex are minor branches which reach the piriform lobe and olfactory tracts. On the border of the old and the new cortex there run the olfactory arteries: rostral and caudal. In European badger the rostral olfactory artery in 6.3% of cases was a vessel which descended independently from the rostral cerebral artery. In the other cases it was a vessel which descended independently from the main trunk of the middle cerebral artery in 18.7% cases and the vessel which got separated with a common trunk with the orbital, ventral and caudal frontal branches.

The caudal olfactory artery, on the other hand, in 20.3% cases was a vessel descending independently from the main trunk. In the other cerebral hemispheres it was one of the branches of the common trunk for temporal branches or descended directly from the ventral temporal branch.

The other cortical branches of the middle cerebral artery can be divided into a group of frontal, parietal and temporal branches. In European badger, similarly as in European otter and other Carnivora species, there occur eight main vessels which supply blood to the same areas of cerebral hemispheres. Respective cortical branches can descend from the main trunk of the middle cerebral artery with a common descent. Such cases of the descent were reported by Chadzypanagiotis (3), Wiland (4) as the rostral, middle and caudal middle cerebral artery. In European badger the rostral middle cerebral artery has been demonstrated as a common trunk for frontal branches and it occurred in 25.0% of the cases investigated, the dorsal middle cerebral artery has been referred to as a common trunk for parietal branches was identified in 14.1% of the cases. The caudal middle cerebral artery

as a common trunk for temporal branches was reported in 20.3% of the cases. In European badger the dorsal middle cerebral artery accounted for the lowest percentage of cases, whereas the rostral middle cerebral artery dominated here. A comparison of the present results with those reported by Skoczylas et al. (8), one can state that also in European otter the dorsal middle cerebral artery accounts for the lowest percentage of cases and the rostral middle cerebral artery – for the highest percentage of cases.

In European badger, similarly as in the mammals investigated, parietal branches are least developed. On the surface of telencephalon the frontal branches of the middle cerebral artery are best developed.

The descriptions of the anatomy of the middle cerebral artery provided in publications of Jabłoński et al. (6), Skoczylas et al. (8) in grivet and European otter show that it is usually a single vessel descending from the rostral cerebral artery. The vessel, having passed the lateral rhinal sulcus, gets divided along its course into respective branches. In the material investigated such a pattern of division of the middle cerebral artery was identified in 93.7% of the cases. In European badger there were found cases of the descent, from the rostral cerebral artery, two independent arterial trunks in 6.3% of the cases. The second independent branch from the rostral cerebral artery was the rostral olfactory artery. In the other mammal species the presence of two independent descends of the branches of the middle cerebral artery from the rostral cerebral artery was reported in domestic rabbit in 31.4% (12) and in raccoon dog (13) w 18,6% of the cases and in wild rabbit (14) – in 36.5% of the cases.

The present research shows that in European badger the observed division of the middle cerebral artery into the same branches or their groups as in the other mammal species studied so far is due to genetic limitations. As claimed by Wiland (15), the blood supply to the brain in the individuals of given species the amount of genetic information accumulated over the phylogenetic development can be essential.

References

- Hofmann M. Zur vergleichenden Anatomie der Gehirn und Ruckenmarksarterien der Vertebraten. *Z Morphol Anthropol* 1900; 2: 247–320.
- Walinczus J. The middle cerebral artery in domestic pig. *Uczen Zap Witebsk Weterinar Inst* 1973; 26: 123–7.
- Chadzypanagiotis D. Arteries on the surface of the cerebral hemisphere in the cat. *Folia Morphol Warsz* 1975; 32: 385–99.
- Wiland C. Comparative investigation of cortical branches of middle cerebral artery in some species of Carnivores. *Zesz Nauk ATR Bydgoszcz* 1991; 44: 1–52.
- Skoczylas B, Wiland C. Cortical branches of the middle cerebral artery in the wild boar (*Sus scrofa L.*). *Electron J Polish Agric Univ Vet Med* 1999; 2(1): e1. <http://www.ejpau.media.pl/volume2/issue1/veterinary/art-01.html>
- Jabłoński R, Skoczylas B, Brudnicki W, et al. Cortical branches of the middle cerebral artery in grivet (*Cercopithecus aethiops*). *Prace Kom Nauk Roln Biol BTN Ser B* 2005; 56: 51–5.
- Skoczylas B, Nowicki W, Jabłoński R, et al. Cortical branches of the middle cerebral artery in yellow baboon (*Papio cynocephalus Linnaeus* 1766). *Prace Kom Nauk Roln Biol BTN Ser B* 2006; 60: 79–84.
- Skoczylas B, Brudnicki W, Nowicki W, et al. The cortical branches of the middle cerebral artery in the otter (*Lutra lutra*). *Vet Med* 2012; 57(6): 282–6.
- Skoczylas B. Cortical branches of middle cerebral artery in domestic pig. (*Sus scrofa f. domestica*). *Electron J Polish Agric Univ Vet Med* 2000; 3: e1. <http://www.ejpau.media.pl/volume3/issue1/veterinary/art-01.html>
- Brauer K, Schaber W. *Katalog der sangtiergehirne*. Jena : VEB Gustaw Fisher, 1970.
- Godynicki S. Use of LBS 3060 Latex in anatomic preparations. *Folia Morphol Warsz* 1971; 30(4): 601–3.
- Wiland C. Basilar arteries of the brain in the domestic rabbit. *Folia Morphol* 1968; 27: 288–95.
- Brudnicki W, Wiland C, Jabłoński R. Basilar arteries of the brain in raccoon dog (*Nyctereutes procyonoides* Grey 1834). *Arch Vet Pol* 1994; 34: 141–7.
- Brudnicki W, Nowicki W, Skoczylas B, et al. Arteries of the brain in wild European rabbit *Oryctolagus cuniculus* (Linnaeus, 1758). *Folia Biol* 2012; 60(3/4): 189–94.
- Wiland C. Variability of the brain base arteries in Canidae and Mustelidae. *BTN Prace Wyzd Nauk Przyr B* 1980; 29: 73–95.

KORTIKALNE VEJE SREDNJE MOŽGANSKE ARTERIJE PRI EVROPSKEM JAZBECU (*MELES MELES*)

B. Skoczylas, W. Brudnicki, K. KirkiŃo-Stacewicz, W. Nowicki, J. Wach

Povzetek: Vzorec in razlike v razvejanosti kortikalnih vej srednje možganske arterije smo preučevali v 64 možganskih poloblah evropskega jazbeca. Ugotovili smo, da se glavna arterija razdeli na deset vedno prisotnih vej. Dve vohalni arteriji oskrbujeta območje možganov, ki se nahaja na meji med področjem neokorteksa in starejšega dela skorje možgan. Preostalih osem vej se deli na triveje, ki se usmerijo v čelno področje, dve veji usmerjeni v parietalno področje in tri senčnične veje, ki oskrbujejo področje neokorteksa. Čelne, parietalne in temporalne veje se spustijo neodvisno od glavnega debla srednje možganske arterije, ali pa najprej oblikujejo skupno deblo. Običajna debla za posamezne skupine vej so opisana kot rostralna, dorzalna in kavdalna srednja možganska arterija. Rostralna vohalna arterija je bila v 6,3 odstotkih preiskovanih primerov neodvisna od rostralne možganske arterije.

Ključne besede: arterije; možgani; evropski jazbec

REDUCING THE NUMBER OF BACTERIAL COLONIES USING ECOCID® S (POTASSIUM PEROXYSULPHATE BASED DISINFECTANT) AT SMALL ANIMAL CLINIC

Nataša Tozon^{1*}, Majda Biasizzo², Leon Ščuka³, Tamara Potočnik³, Marjeta Redek³, Luka Prem³

¹Small Animal Clinic, ²Institute of Food Safety, Feed and Environment, Veterinary Faculty, University of Ljubljana, Gerbičeva 60, 1000 Ljubljana, ³Krka, d. d., Šmarješka cesta 6, 8501 Novo mesto

*Corresponding author, E-mail: natasa.tozon@vf.uni-lj.si

Abstract: A clinical study has been conducted to test the efficacy of Ecocid® S, a biocidal agent. The active substance is potassium peroxy sulphate and is used in clinical practice after the mechanical cleaning of various surfaces that act as potential sources of infection transmission. We determined 29 swabbing points, from which 87 samples were collected with cotton swabs. Swabs were submitted for microbiological testing to evaluate microbial contamination before cleaning, and before and after disinfection with Ecocid® S. We submitted 63 swabs from 21 swabbing points for further statistical analysis. Five swabs were excluded because the presence of bacteria in the swabs before disinfection had not been determined. The clinical study on the efficacy of Ecocid® S disinfectant showed that it is effective with an average reduction in contamination of 95.75%. The disinfectant was also active with a significantly reduced time of action: it was removed with dry paper towels from all sampling points, except the floor scales, only 5 to 10 minutes after application. The time required for the proper preparation of examination tables and other equipment in clinical practice is of vital importance for a smooth workflow.

Key words: animals; disinfection; potassium peroxy sulphate; Ecocid® S

Introduction

The standard cleaning protocol is applied at Small Animal Clinic to maintain suitable hygiene conditions following the professional recommendations and good clinical practice (1). All surfaces should be made of materials suitable for cleaning with disinfectants and for mechanical wet cleaning to prevent transmission of pathogens from one patient to another, and in case of zoonoses, from animal patients to humans.

A clinical study has been conducted at the Small Animal Clinic to test the biocidal agent Ecocid® S in clinical conditions. Ecocid® S belongs to a group of oxidising disinfectants. Different studies have confirmed the efficacy and safety of Ecocid® S under laboratory conditions^{4,5}(2).

The active substance of Ecocid® S is potassium peroxy sulphate. Its efficacy is increased by added surfactants, organic acids and an inorganic buffer system. It has been proven effective against many infectious microorganisms such as viruses, bacteria and fungi (3, 4, 5, 6, 7). Because of its special composition, Ecocid® S guarantees good contact with the cell surface and acts on most cell elements, the cytoplasmic membrane, the cytoplasm and the nucleus. By acting on the nucleus, it causes the destruction of the pathogen's genetic material and therefore prevents horizontal and vertical disease transmission (8).

⁴Zorman Rojs O. Ugotavljanje virucidnega delovanja Ecocid® S na virus aviarne influence H5N1, laboratorij za kužne bolezni perutnine, Univerza v Ljubljani, Veterinarska fakulteta, Ljubljana, 2006

⁵Zorman Rojs O. Comparative testing of the efficacy of the disinfectant Ecocid® S against gumboro disease virus isolates of different pathogenicity, Institute for poultry health and protection, University of Ljubljana, Veterinary faculty, Ljubljana, 2007.

The study aimed to confirm the efficacy and safety of Ecocid® S in clinical conditions at small animal clinic using the standard protocol of cleaning and disinfection of the most exposed areas of the clinic.

Material and methods

Cleaning and disinfection procedure

The mechanical cleaning procedure for all selected surfaces was carried out according to the operating procedure of the clinic, based on the good clinical practice and according to FECAVA Key Recommendations for Hygiene and Infection Control in Veterinary Practice (1). Potentially critical sites as regards microbial contamination and possible transmission routes of infections were determined and included in the study. After mechanical cleaning with a neutral detergent solution with water and paper towels, the surface of each item was disinfected with freshly prepared 1% Ecocid® S solution, according to the recommendations of the manufacturer (9). Approximately 100 ml of the solution per m² was used and left to act for approximately 5–10 minutes. Only the floor scale had a 30-minute contact time.

Sampling

A sterile cotton bud was dipped into a tube of 5 ml 0.1% peptone salt solution (Proteose Peptone 1.0 g/L (Biolife Italiana Srl, Milan, Italy), NaCl 8.5 g/L (Merck KGaA, Darmstadt, Germany)). The surface of each 20 cm² marked spot was swabbed in two directions. A sample was taken immediately before and after sanitation (cleaning, disinfection) from each sampling site. After disinfection, each sampling site was dried with paper towels before swabbing to neutralise any biocidal residues on the surface and to prevent any further biocidal action on microorganisms in the samples before the laboratory analysis. After sampling, the swabs were refrigerated and brought to the laboratory within two hours of collection.

Sampling sites were determined according to the highest exposure rate of the equipment (Table 1).

Microbiological method

The method for the enumeration of microor-

ganisms was used to evaluate the surface contamination levels before cleaning and before and after disinfection. Swab samples were homogenised, diluted where needed and inoculated into Petri dishes. Non-selective solid medium (Tryptic glucose yeast agar, Biolife) was poured, allowed to solidify and then incubated for 72 hours at 30 °C. A sample with a known concentration of *Bacillus subtilis* subsp. *spizizenii* WDCM 00003 was tested in parallel to other samples as a quality control. Results were calculated based on counted colonies and expressed as the number of colony forming units per 20 cm² (CFU/area).

Data processing and report preparation

Basic statistical methods were applied in data processing (calculation of percentages-reduction of number of microorganisms), and the following tests were applied in data analysis: the χ^2 test (chi-squared test) for the comparison of the number of swabs based on the given criteria (80% reduction and 95% reduction of microorganisms). The number of microorganisms after cleaning and after disinfection were compared. Before the data were processed, values for total colony forming units were converted to logarithmic values. Analysis of variance (ANOVA) and the t-test were used to establish the difference between group means. Tukey's test was applied if differences between group means were statistically significant.

Results

We presented Ecocid®S action test results by individual swabbing sites (Table 1). The effectiveness of disinfection was evaluated according to the difference between the evaluated contamination (CFU/20 cm²) before cleaning and before and after disinfection expressed in logarithmic values (\log_{10}) and percent. When reduction was $\geq 1.0 \log_{10}$ CFU/20 cm², contamination decreased by 90.0% or more. If reduction was $\geq 2.0 \log_{10}$, the drop was at least 99.0%, while the 99.99% or more decrease was recorded for reductions $\geq 3.0 \log_{10}$.

The staff collected 87 swab samples from 29 swabbing points. Of these, 63 swabs from 21 swabbing points were submitted to the ensuing statistical analysis. Five swabs were not included in the statistical analysis because the presence of bacteria

Table 1: Source data – number of microorganisms (CFU/20 cm²) for swabbing points and testing phases

Disinfection area	Sample	1	2	3
Cage top panel, presurgical room	1	0	0	0
Cage top grate, presurgical room	2	65	1200	10
Cage bottom panel, presurgical room	3	0	4600	0
Cage bottom floor, presurgical room	4	600	3000	25*
Cage bottom floor (cat), hospital	16	220	2300	0
Cage bottom panel (cat), hospital	17	15*	6000	0
Cage bottom floor (dog), hospital	18	150000	12000	10*
Cage bottom panel (dog), hospital	19	2300	85000	10*
Examination table, cardiology ultrasound	5	25*	40*	0
Table, surgery room no. 3	6	65	2200	0
Table, presurgical room	7	15*	15000	0
Table, dentistry	8	0	15000	0
Examination table, exam room no. 106	20	15*	6000	0
Examination table, hospital	21	180	85	0
Examination table, ultrasound	24	460	0	0
Examination table, X-ray room	26	55	10*	10*
Examination table, dermatology room	29	1400	15000	20*
Transport table	25	450	30*	0
Thermophore (cat)	12	15*	0	0
Thermophore (dog)	28	140	25*	20*
Scale, reception	14	950	2300	60
Scales, exam room	15	550	8000	0
Inhalation chamber, panel	22	1100	15	0
Inhalation chamber, connectors	23	0	0	0
Laminar airflow bench for preparing cytostatic agents	27	40	15000	15
Tracheal tube (cat), orthopaedic	9	750	0	0
Tracheal tube (dog), dentistry	10	85	10	0
Tracheal tube (dog), orthopaedic	11	0	0	0
Tracheal tube (cat)	13	20*	0	0

Legend:

1 – Number of microorganisms before cleaning (CFU/surface)

2 – Number of microorganisms before disinfection (CFU/surface)

3 – Number of microorganisms after disinfection (CFU/surface)

* - Estimated number – low counts (< 10 CFU/plate) - precision of the result is low and the result is reported as estimated

Note regarding the 0 value: Number of microorganisms < 5 CFU/surface (values under the detection limit) were regarded as 0.00

in the swabs before disinfection had not been determined (< 5 CFU/surface). The number of microorganisms was converted to logarithmic values. For statistical processing, results reported as < 5 CFU/surface, i.e. below the detection limit, were assigned a value of 0.00 log₁₀, corresponding to 1 CFU.

Swabs collected from cages showed that the average decrease in the contamination level after disinfection was statistically significant at 99.64% (P < 0.01). The differences in contamination lev-

el before cleaning and after disinfection were also statistically significant (P = 0.006). Swabs collected from tables showed that the number of microorganisms after disinfection decreased on average by 88.87%. Reduction in contamination after disinfection compared to before disinfection was statistically significant (P < 0.001). Reduction in contamination after disinfection in comparison to the number of microorganisms before cleaning was also statistically significant (P = 0.004).

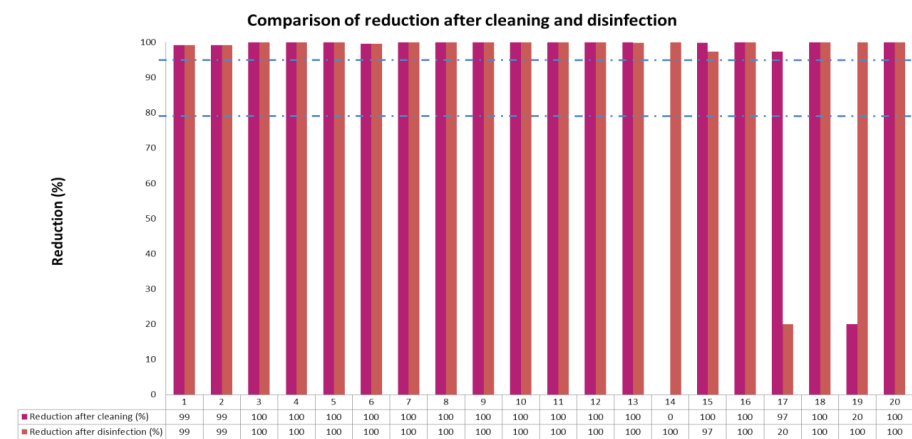


Figure 1: Reduction in contamination (%) after cleaning and after disinfection on all tested surfaces

The number of microorganisms after disinfection of tracheal tubes decreased on average by 100%. Reduction in contamination after disinfection in comparison to the level before cleaning ($P = 0.011$) indicated that the complete sanitation procedure was effective.

Results of the swabs collected from scales showed a reduction in contamination levels after disinfection, but due to the small number of samples, it could not be proven statistically. Swabs collected from only two thermophores showed that cleaning reduced the number of microorganisms: in one case contamination levels after cleaning diminished completely and in another significantly. Comparison of contamination levels before cleaning and after disinfection indicated that cleaning had a significant impact on the entire sanitation procedure. Swabs collected from other equipment (an inhalation chamber panel and a biological safety cabinet for preparation of cytostatic agents) showed that the number of microorganisms after using Ecocid® S decreased on average by 100% (an inhalation chamber), and by 99.90% (a laminar flow).

According to the statistical analysis of 21 swabs out of total 24, it appears that the decrease in contamination level after disinfection was statistically significant ($P < 0.05$). Three samples were excluded because all microorganisms had already been removed by cleaning. Contamination after disinfection was reduced by 91.2% (SE = 5.9%) on average compared to contamination after cleaning. In one instance (a thermophore used in dogs) contamination after cleaning was reduced by 0% in comparison to disinfection. In this case, the number of microorganisms was very low (25 after cleaning, and 20 after disinfection), even though

this may be attributed to the uneven surface of the thermophore, which features a ribbed rubber design. In 20 remaining swabs, contamination was reduced by almost 96% (95.75%).

There were no statistically significant ($P = 1.00$) differences between the compared criteria of reduction effectiveness (95% or 80%) regarding the number of microorganisms (Figure 1).

Discussion

The investigation showed that Ecocid® S is effective in clinical conditions if cleaning and disinfecting protocols applicable at the clinic are followed and if the preparation is made in accordance with professional guidelines and good clinical practice (1). Microbial contamination decreased on average by 91.2% after disinfection with Ecocid® S, which is comparable with previous findings^{6,7,8,9}. This represents a statistically significant reduction at $P < 0.05$, which was also confirmed by separate analyses for individual sampling points on cages, examination tables, and tracheal tubes. Cages and tables are made of stainless steel and the removable sub-floor grate is plastic-coated, so all surfaces are smooth and good hygiene is already maintained with mechanical cleaning. In certain cases, the number of microorganisms went up, which

⁶Ščuka L. Statistical analysis of the efficacy and safety study of the Ecocid® S in comparison with reference product, Ljubljana, 2008. Report: 1–10.

⁷Juršič R, Ščuka L. Ugotavljanje učinkovitosti dezinficijsnega Ecocid® S v praktičnih pogojih na perutninskih farmi. Report: 1–7.

⁸Poročilo o testu delovanja biocidnega sredstva Ecocid® S v prašičerejskem objektu, Univerza v Ljubljani, Veterinarska fakulteta, February 2007.

⁹Gruntar I. Poročilo o baktericidni aktivnosti (prEN 1656) produkta Ecocid® S, Inštitut za mikrobiologijo in parazitologijo, Univerza v Ljubljani, Veterinarska fakulteta, Ljubljana 2007.

could be attributed to using the cleaning agent in a sprayer. It is possible that the spray, which includes microorganisms, forms an aerosol that settles on the surface again. Contamination can therefore only be reduced by applying a disinfectant. Even though we removed the disinfectant with dry paper towels within 5 to 10 minutes after spraying, it obviously acted long enough to achieve the required result. The suggested exposure of the disinfectant used in the study is 30 minutes (9). We believe that the reduced time of action is exceptionally important for clinical practice, because it allows for much faster patient flow and a smooth workflow.

Ecocid®S is an effective biocide and can also be used for tracheal tubes of smooth non-porous plastics after cleaning by rinsing with drinking quality water. We believe that any residual disinfectants used for disinfection of tracheal tubes coming in direct contact with the mucous surface of the respiratory tract should be removed thoroughly with drinking quality water.

Differences in results of swabs collected from scales were considerable and can be considered significant, although the swabs were only collected from two scales. Cleaning and disinfection were slightly less effective with the floor scale, which was expected because of its non-slip PVC lining with a rough textured surface compared to table scales, whose surface is made of smooth plastic material. Cleaning of floor scales generally takes place twice a day and more often if patients discharge (defecate, urinate, or vomit) on the device. More microorganisms from soiling are expected to accumulate on the lining, which cakes after a while. Only when this had happened, did we leave the disinfectant to act for 30 minutes. However, the extended time period was not sufficient to eliminate the presence of microorganisms. We believe that the extended time of action helped dissolve caked soiling, because the preliminary mechanical cleaning protocol was the same as with smooth surfaces. To reduce contamination more efficiently, it would be necessary to optimise mechanical cleaning. We nevertheless believe that the disinfection protocol for the floor scales is satisfactory because patients generally only stand on the lining. This does not represent a major hazard if the number of microorganisms is as low as established during our investigation. We obtained similar results using the same cleaning and disinfection protocol on thermophores,

which are often used with patients during and after general anaesthesia. Direct contact with patients is generally avoided when using thermophores. Because their surface is uneven, they must be appropriately cleaned whenever they come into contact with a patient, with drinking quality water and disinfectant. To remove any residual disinfectant that might potentially cause irritation, it is recommended that they are rinsed with drinking quality water after disinfection.

Analysis results of other sampling points (the inhalation chamber and the biological safety cabinet for preparation of cytostatic agents), selected as a potential source of transmission of pathogens also show that cleaning and disinfection procedures were appropriate.

Efficacy of Ecocid® S biocidal preparation in practical clinical conditions at the Small Animal Clinic in all places at the structure and on all selected surfaces fully met the required performance threshold of decreasing contamination on average by 1 log₁₀ CFU/20 cm² (i.e. the contamination level was reduced at least by 90%). There are limited data on hospital-associated infections and only a few studies on optimal cleaning and disinfection procedures in small animal clinical practice (10, 11).

An important limitation of the study is that we did not have the opportunity to test the efficacy on selected and important pathogens, although the product was tested on some of these in laboratory conditions.

Conclusion

The study showed that Ecocid® S disinfectant is effective in practical clinical conditions with an average 95.75% reduction in microorganisms compared to samples before and at the end of the disinfection process. The disinfectant was also effective when the time of action was significantly shorter, as it was wiped clean with dry paper towels from all sampling points except the floor scales only 5 to 10 minutes after application. The time needed for the entire process of proper disinfection between individual patients is of utmost importance for a smooth clinical workflow. We believe that Ecocid® S can be successfully used even for the same equipment, such as tracheal tubes. When it is rinsed off with drinking quality water, it does not cause any irritation in animals.

Acknowledgements

The study was supported by Krka, d. d., Novo mesto, Slovenia, including English language editing by a professional English proof-reader.

References

1. FECAVA key recommendations for hygiene and infection control in veterinary practice. https://www.fecava.org/wp-content/uploads/2019/03/FECAVA_Infectioncontrol_2018_LR.pdf (28. 7. 2019)
2. Yilmaz A. Test report, prEN 14675, virucidal activity (obligatory and optional conditions). Gießen : Klinik für Vögel, Reptilien, Amphibien und Fische, Justus-Liebig-Universität Gießen, 2006.
3. Sonthipet S, Ruenphet S, Takehara K. Bactericidal and virucidal efficacies of potassium monopersulfate and its application for inactivating avian influenza virus on virus-spiked clothes. *J Vet Med Sci* 2018; 80(4): 568–73.
4. Addie DD, Boucraut-baralon C, Egberink H, et al. Disinfectant choices in veterinary practices, shelters and households: ABCD guidelines on safe and effective disinfection for feline environments. *J Feline Med Surg* 2015; 17(7): 594–605.
5. Moriello KA. Kennel Disinfectants for *Microporum canis* and *Trichophyton sp.* *Vet Med Int* 2015; 2015: e853937. doi: 10.1155/2015/853937
6. Eleraky NZ, Potgieter LN, Kennedy MA. Virucidal efficacy of four new disinfectants. *J Am Anim Hosp Assoc* 2002; 38(3): 231–4.
7. Matsuoka T, Yoshida S, Ohashi K, et al. Evaluation of efficacy and clinical utility of potassium peroxymonosulfate-based disinfectants. *Can J Infect* 2018; 32(2): 93–7.
8. Pentapotassium bis(peroxymonosulphate) bis(sulphate). European Chemical Agency ECHA. <https://echa.europa.eu/registration-dossier/-/registered-dossier/15990> (30. 4. 2018)
9. Ecocid® S. Summary of product characteristics. Novo mesto, Slovenija : Krka d. o. o., 2017: 1–4.
10. Stull JW, Weese JS. Hospital-associated infections in small animal practice. *Vet Clin North Am Small Anim Pract* 2015; 45: 217–33.
11. Traverse M, Aceto H. Environmental cleaning and disinfection. *Vet Clin North Am Small Anim Pract* 2015; 45: 299–30.

ZMANJŠANJE ŠTEVILA BAKTERIJ PO UPORABI RAZKUŽILA ECOCID® S (RAZKUŽILO NA OSNOVI KALIJEVEGA PEROKSISULFATA) V PROSTORIH KLINIKE ZA MALE ŽIVALI

N.Tozon, M. Biasizzo, L. Ščuka, T. Potočnik, M. Redek, L. Prem

Povzetek: S klinično študijo smo želeli ugotoviti učinkovitosti biocidnega razkužila Ecocid® S. Aktivna snov v razkužilu je kalijev peroksisulfat, ki se na klinikah uporablja za razkuževanje različnih površin, ki predstavljajo ključna mesta za prenos okužb, po njihovem mehaničnem čiščenju. Določili smo 29 vzorčnih mest, na katerih smo z uporabo bombažnih brisov odvzeli 87 vzorcev. Z mikrobiološkim testiranjem smo ugotavljali stopnjo kontaminacije pred čiščenjem, ter pred in po razkuževanju z Ecocid® S. Za statistično obdelavo smo uporabili 63 rezultatov z 21 vzorčnih mest. Pet rezultatov je bilo izločenih iz obdelave, ker je bila že pred razkuževanjem stopnja kontaminacije pod mejo detekcije uporabljene metode. S klinično študijo učinkovitosti razkužila Ecocid® S smo ugotovili povprečno 95,75 % zmanjšanje števila kontaminantov po uporabi razkužila. Razkužilo je bilo učinkovito tudi ob skrajšanem času delovanja le 5 do 10 minut po nanosu. Zaradi zagotavljanja tekočega dela na kliniki je izredno pomemben čas, ki je potreben za ustrezno pripravo površin in druge opreme za pregled živali, zato je razkužilo Ecocid® S primerno za uporabo na veterinarskih klinikah, saj hitro in učinkovito zmanjša bakterijsko kontaminacijo.

Ključne besede: živali; dezinfekcija; kalijev peroksisulfat; Ecocid® S

OCCURRENCE, MOLECULAR IDENTIFICATION AND ANTIBIOTIC RESISTANCE PROFILING OF *MYCOPLASMA GALLISEPTICUM* AND *MYCOPLASMA SYNOVIAE* FROM CHRONIC RESPIRATORY DISEASE CASES IN POULTRY BIRDS AND FARM ENVIRONMENT

Abu Baker Siddique^{1*}, Sajjad Ur Rahman², Mazhar Ulhaq³, Rasheeha Naveed²

¹Department of Microbiology, Government College University, Faisalabad-Pakistan 38000, ²Institute of Microbiology, University of Agriculture, Faisalabad-Pakistan, 38040, ³Department of Veterinary Biomedical Sciences, Faculty of Veterinary and Animal Sciences, PMAS, Arid Agriculture University, Rawalpindi, Pakistan 46300, Pakistan

*Corresponding author, E-mail: absiddique@gcuf.edu.pk

Abstract: Avian mycoplasmosis is an important risk for commercial poultry production leading to enormous losses in terms of disease and productivity. The main causative agents are *Mycoplasma gallisepticum* and *Mycoplasma synoviae*. To study the variable degree of resistance to commonly prescribed and used antibiotics in mycoplasmosis, a total of 115 samples including tissue specimen and swabs were collected from chronic respiratory disease (CRD) cases of broiler and layer birds and their contaminated farm environment. The samples were directly passaged into the Brain Heart Infusion broth (supplemented with 10 % horse serum, NAD, cysteine, penicillin and thallium acetate). Positive samples were transferred to Brain Heart Infusion agar (Difco) for the isolation of *Mycoplasma* spp. while negative samples were declared after the third passage. Of the samples, 61.5% were found positive for *Mycoplasma* spp., which were recovered mostly after second passage. Out of total culture positive cases, *Mycoplasma gallisepticum* (MG) was identified in 62% cases and *Mycoplasma synoviae* (MS) in 38%, as confirmed through Polymerase Chain Reaction (PCR) using specific primers. The MG and MS isolates showed variable degrees of sensitivity against the commercially available drug of choice, tylosin. The highest Minimum Inhibitory Concentration (MIC) of enrofloxacin ($112.38 \pm 4.34 \mu\text{g/ml}$) was recorded against MG, followed by tetracyclin ($91.58 \pm 4.66 \mu\text{l/ml}$), gentamicin ($54.33 \pm 2.98 \mu\text{g/ml}$), spiro-mycin ($52.23 \pm 3.99 \mu\text{g/ml}$) and tylosin ($52.58 \pm 2.69 \mu\text{g/ml}$). The highest MIC for enrofloxacin ($168.24 \pm 3.82 \mu\text{g/ml}$) was recorded against MS followed by tetracyclin ($115.48 \pm 2.62 \mu\text{g/ml}$), spiro-mycin ($95.96 \pm 2.17 \mu\text{g/ml}$), tylosin ($84.84 \pm 2.56 \mu\text{g/ml}$) and gentamicin ($46.4 \pm 2.18 \mu\text{g/ml}$). Multiplex PCR is a time tested tool for the molecular diagnosis and confirmation of *Mycoplasma* species.

Key words: avian mycoplasmosis; chronic respiratory distress; minimum inhibitory concentration; multiplex polymerase chain reaction

Introduction

Mycoplasma infections continue to be an important cause of loss in poultry production. The economic consequences are important because of decreased egg production; and growth, and poor hatchability rates due to increased embryo mortality and account for 5-10% of early chick mortality

(1, 40). Mycoplasmosis results in reduced weight gain and feed conversion efficiency along with significant downgrading of carcasses at slaughter due to airsacculitis and arthritis lesions (2, 3). Mycoplasmosis is thus a major problem for the poultry industry; and the infections are commonly known as Chronic Respiratory Disease (CRD) of chickens and infectious sinusitis of turkeys (4).

Mycoplasma gallisepticum (MG) is an economically significant pathogen of poultry; and the World Organization of Animal Health (OIE), has declared

the disease caused by MG as notifiable (1). *Mycoplasma synoviae* (MS) infection most frequently occurs as sub-clinical upper respiratory problem, and causes air sac lesions when combined with Newcastle Disease, Infectious Bronchitis, or both (5, 6). Systemic *M. synoviae* infection results in synovitis, an acute to chronic disease of chickens and turkeys, involving the synovial membrane of joints and tendon sheaths (7, 8). In recent reports, *Mycoplasma synoviae* has also been diagnosed as a causative agent of an emerging issue of sharp decline in egg production with eggshell apex abnormalities in poultry (9, 41).

In view of the forthcoming World Trade Organization (WTO) recommendations, the establishment of *Mycoplasma*-free chickens, day old chicks and hatching eggs is needed; otherwise exports will be impossible (10). Control of *Mycoplasma* infections by vaccination is possible, and various measures are implemented in many countries and control and eradication programs, particularly for MG in breeding stock, are successful. Sometime, chemotherapeutic approaches become necessary to minimize *Mycoplasma* transmission in cases of outbreaks, as a complement to bio-security measures, in order to minimize economic losses as well as lateral and vertical transmission (8).

Many antimicrobial drug groups, such as macrolides, pleuromutilins, tetracyclines and fluoroquinolones, have been shown to possess inhibitory activity against various mycoplasmas in *in-vitro* studies (11). However, an increase in resistance of *Mycoplasma gallisepticum* against tetracyclines (12, 13), macrolides (14, 15) and quinolones (16) has been reported and treatment strategies have proved unsatisfactory (17).

The current study was aimed at the isolation molecular identification and antibiotic resistance profiling of MG and MS from commercial poultry birds (broilers and layers) and the farm settings/ environment.

Materials and methods

Sample collection

A total of 115 samples were collected; most from diseased but alive broiler and layer birds showing signs of respiratory distress and other clinical signs were (n=94), and the rest from contaminated farm environments (n=21). Samples from birds included tissues such as trachea and lungs,

exudates from air sacs and oral swabs, as well as synovial fluids, while samples collected from farm environment were only swabs from building walls, water drinkers and feeders (18).

Isolation of Mycoplasma species

The samples were directly inoculated into modified Brain heart infusion (BHI) broth (Difco TM Detroit, United States) as described previously (3), supplemented by 10% horse serum, NAD, cysteine chloride, penicillin, thallium acetate and phenol red. The samples were incubated at 37 °C for 24-72 hours. The negative samples (showing no growth) were further passaged while positive samples were transferred to Brain Heart Infusion agar (Difco) for the successful isolation of *Mycoplasma gallisepticum* and *Mycoplasma synoviae*. The isolate identifications were confirmed by the biochemical tests; glucose fermentation, arginine hydrolysis, phosphatase activity, film and spot production, tetrazolium reduction and casein digestion (19, 20).

Molecular confirmation

The DNA from the isolated *Mycoplasma* spp. was extracted and purified using Phenol Chloroform method (21). The isolated DNA was subjected to multiplex Polymerase Chain Reaction (PCR) using specific primer sequences (22). For MG, the lipoprotein gene was amplified using primer MG-F 5'-GGATCCCATCTCGACCACGAGAAAA-3' and MG-R 5'-CCTTCAATCAGTG: AGTAACTGATGA -3' and for MS, the 16SrRNA gene was targeted using primer MS-F 5'- GAA GCAAATAGTGATATCA- 3' and MS-R 5'- GTCGTCTCGAAGTTAACAA - 3'. The PCR was performed using 50 µl of master mix (Vivantis, USA) and 10 pM of each forward and reverse primer. The reaction protocol was optimized as: initial denaturation at 94 °C for five minutes, followed by 30 cycles of denaturation at 94°C for 45 sec, annealing at 50 °C for 30 sec, and extension at 72 °C for 1 min, while final extension was done at 72 °C for 7 min in thermal cycler (PqLab, Germany). The amplified product was run on 2% agarose gel using 0.2 µg/ml ethidium bromide dye and visualized in gel documentation system (Dolphin Doc, USA) using a 100bp ladder (Vivantis, USA) as DNA marker (23).

Determination of minimum inhibitory concentrations

The isolates were subjected to a broth micro-dilution technique to determine the Minimum Inhibitory Concentrations (MICs) as described previously (12, 24, 25). Five antibiotics were selected representing different antibiotic classes: enrofloxacin, tetracycline, gentamicin, spiroomicin, and tylosin. The assay was performed in 96-well micro-titration plates. Two-fold serial dilutions of the different antibiotics, were made in 50 μ l modified BHI broth. At the end, 150 μ l of broth containing organisms (10^4 - 10^5 CFU/ml) was added into each well. Two parallel controls were also run, including a control positive (Culture control) containing broth and test culture, and a control negative containing no antibiotic. The minimum concentration of antibiotic that prevented the color change of the medium was taken as the MIC (15, 26).

Statistical analysis

Antimicrobial sensitivity of different types of isolates collected from different types of farms against different types of antibiotics makes a complex design of experiment. Descriptive statistics are presented as the mean of MIC values for different types of isolates for each antibiotic with standard deviation (Table 1). MIC values for both species against similar antibiotics were compared with one-way analysis of variance (ANOVA) and student t-test, with a significance level of 0.05.

In addition, data for each *Mycoplasma* spp. were analyzed separately with one-way ANOVA at a significance level of 0.01. All data analyses were done by using Minitab® version 16 (Minitab Inc.).

Results

Isolation of mycoplasma

Of the 115 samples collected from chronic respiratory disease cases of broiler and layer birds, 61.5% were positive for *Mycoplasma* spp. Of these positive cultures, 62% were positive for *Mycoplasma gallisepticum* (MG) and 38% for *Mycoplasma synoviae* (MS). MG was isolated from tracheae (40%), air sacs (27%), lungs (10%), oral swabs (10%), feeders /drinkers (8%), and walls (5%) (Figure 1). MS was isolated from synovial fluid (40%), lungs (24%), air sacs (16%), tracheae (12%), and feeders / drinkers (8%) (Figure 2).

Maximum recovery of MG from clinically ill birds was observed from tracheas (42 %) and air sacs (29%), followed by lungs (8%) and oral swabs (8%), whereas recovery from the contaminated farm environment was recorded as 8% from feeder / drinker samples and 4% from wall samples. In the case of *Mycoplasma synoviae*, highest recovery was obtained from synovial fluid (40%) followed by lungs (27%), air sacs (13%), tracheae (13%) and feeder / drinker samples (7%).

The isolates were confirmed through PCR. *Mycoplasma gallisepticum* yielded 720bp of PCR product, while 207 bp band size was observed in case of *Mycoplasma synoviae* (Figure 3).

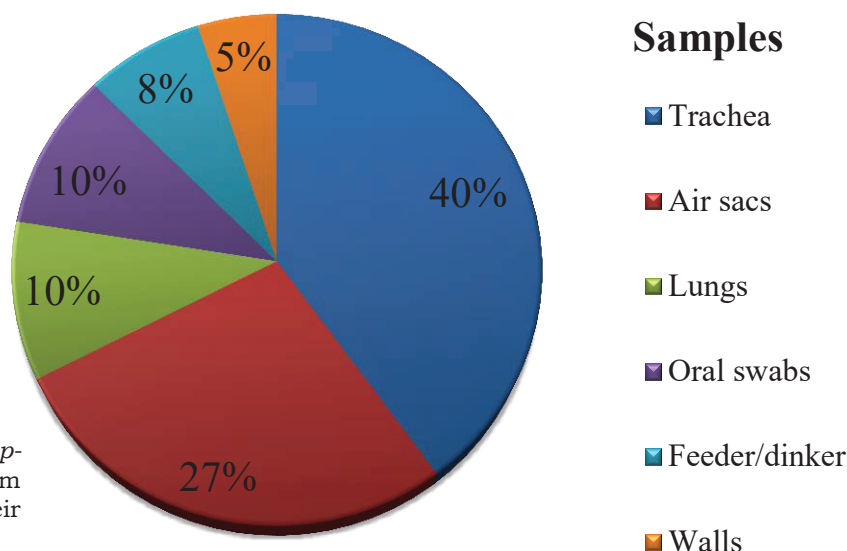


Figure 1: Isolation of *Mycoplasma gallisepticum* from different samples collected from broiler and layered birds as well as their farm environment

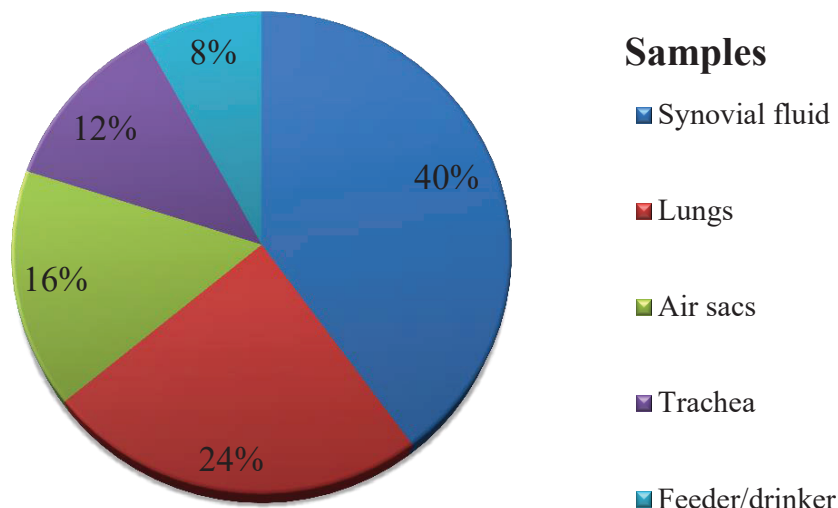


Figure 2: Isolation of *Mycoplasma synoviae* from broiler and layered birds

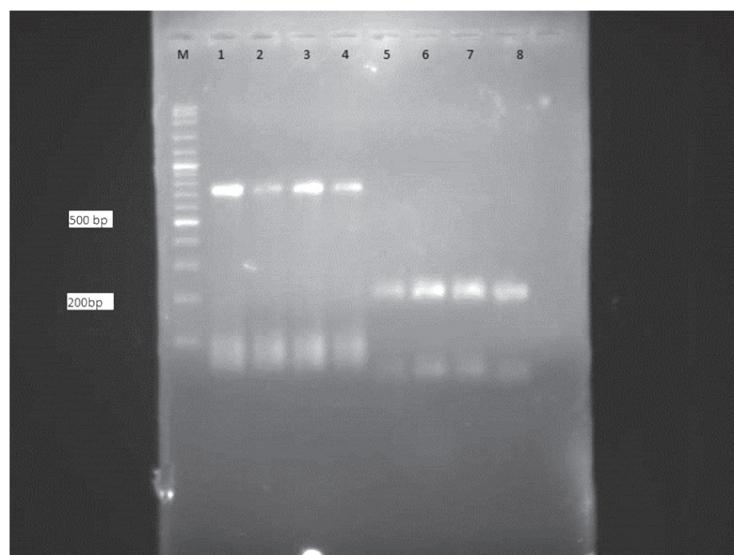


Figure 3: PCR-based confirmation of isolates. Lane M: Marker 100bp, Lane 1, 2, 3 and 4: positive samples for *Mycoplasma gallisepticum*, Lane 5, 6, 7 and 8: positive samples for *Mycoplasma synoviae*

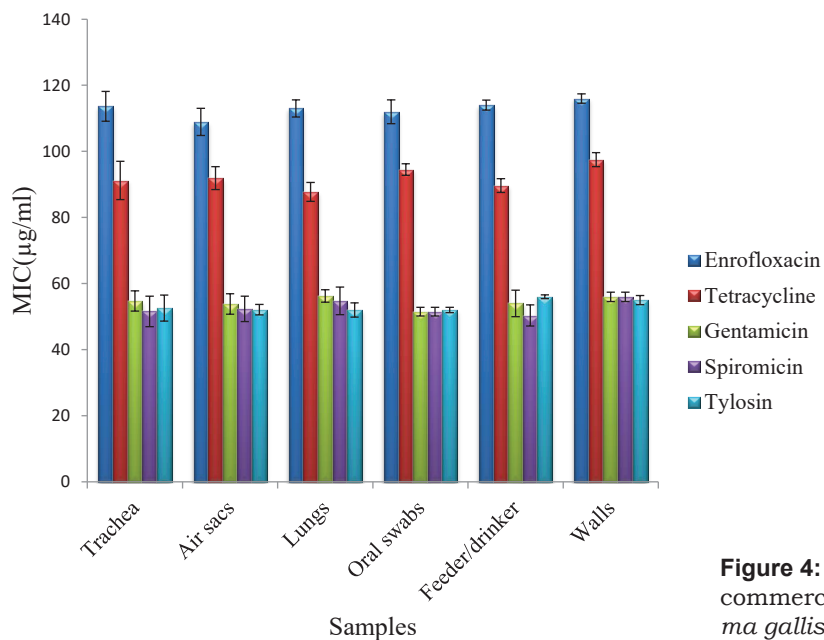


Figure 4: Minimum Inhibitory Concentration (MIC) of commercially available antibiotics against *Mycoplasma gallisepticum* isolated from different samples

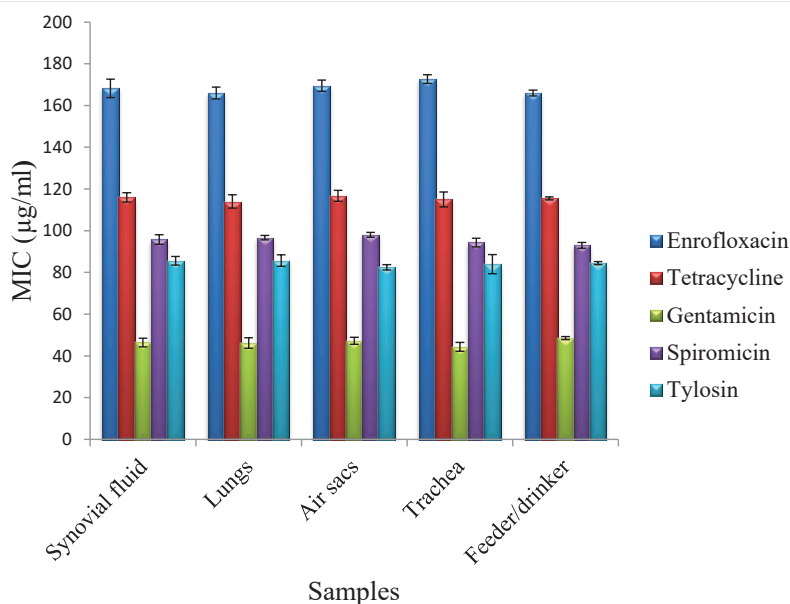


Figure 5: Minimum Inhibitory Concentration (MIC) of commercially available antibiotics against *Mycoplasma synoviae* isolated from different samples

Antibiotic sensitivity profile

The isolates of *Mycoplasma gallisepticum* showed a variable degree of resistance against the antibiotics tested with significantly higher MIC₅₀ of enrofloxacin as compared to the other antibiotics tested (Table 1). Enrofloxacin was followed by tetracycline, gentamicin, spiromycin and tylosin.

In the case of *Mycoplasma synoviae* (MS), significantly higher MIC was also recorded against enrofloxacin. This was followed by tetracycline followed by, spiromycin, tylosin and gentamicin (Table 1).

One way analysis of variance (ANOVA) showed statistical differences ($P < 0.05$) in the MIC of enrofloxacin, tetracycline, gentamicin, spiromycin

and tylosin against MG and MS (Table 1). Statistical analysis with student t-tests ($P < 0.05$) showed that enrofloxacin, tetracycline, spiromycin and tylosin have greater MIC against MS, while gentamicin has greater MIC against MG.

One-way analysis of variance (ANOVA) showed no significant difference ($P < 0.01$) in MIC of enrofloxacin against different isolates of MG. Tetracycline, gentamicin, spiromycin and tylosin also showed the same pattern for different isolates of MG (Figure 4). There were no significant differences ($P < 0.01$) in the MIC of enrofloxacin against different isolates of MS. Tetracycline, gentamicin, spiromycin and tylosin also showed the same pattern for all isolates of MS.

Table 1: Minimum Inhibitory Concentration (MIC) of commercially available antibiotics against *Mycoplasma gallisepticum* and *Mycoplasma synoviae*, shown as (Mean±SD) µg/ml

Antibiotics	<i>Mycoplasma gallisepticum</i> (n=40)	<i>Mycoplasma synoviae</i> (n=25)	P-value
Enrofloxacin	112.38±4.34	168.24 ±3.82	0.00
Tetracycline	91.58±4.66	115.48±2.62	0.00
Gentamicin	54.33±2.98	46.4±2.18	0.00
Spiromycin	52.23±3.99	95.96 ±2.17	0.00
Tylosin	52.58±2.69	84.84±2.56	0.00

Means are significantly different ($P < 0.05$)

Discussion

The disease caused by *Mycoplasma gallisepticum* and *Mycoplasma synoviae* is known as Chronic Respiratory Distress (CRD), which causes heavy economic losses in the poultry industry by decreasing production and increasing the cost of production via medication expenses (10).

A multiplex PCR has been optimized for successful detection of five of the respiratory tract pathogens including *Mycoplasma gallisepticum*, *Mycoplasma synoviae*, Newcastle Disease virus, Infectious Bronchitis virus and Avian Influenza virus (23, 27, 28, 29). Several studies have shown successful detection of individual pathogens, including a multiplex PCR for the detection of *Mycoplasma* spp. (30) and multiplex RT-PCR for respiratory tract viruses (6).

A PCR assay for detection of the variable hemagglutinin gene (*vlhA* gene) of *M. synoviae* (31, 32) has proved to be a useful tool in the detection and typing of different MS strains. Comparing *vlhA*-PCR with *16SrRNA*-PCR (31) has also shown that in the very early stage of infection the *16SrRNA* procedure is more sensitive than the *vlhA* method (27).

The development of multiplex PCR for the detection of different pathogenic species of avian mycoplasma in a sample. The above approach is reliable, sensitive and specific and help to reduce the losses due to mycoplasma infections by early and accurate diagnosis of avian mycoplasma species (22, 24, 25).

The aim of this study was to assess the *in vitro* antimicrobial susceptibilities of *M. gallisepticum* and *M. synoviae* isolates from broilers, layer birds and the farm premises. In Pakistan, the control strategy for avian mycoplasmosis is largely based on the use of effective antibiotics, which helps in controlling the severity of clinical disease and prevents substantial economic losses. However, it is worth mentioning that administration of antibiotics depends on the dosage and duration of administration; which may fail to completely eradicate these pathogens from the infected flocks.

Mycoplasma gallisepticum and *Mycoplasma synoviae* have shown sensitivity *in vitro* to several antimicrobials including, tetracyclines, macrolides, lincosamides, fluoro-quinolones and others (14). PCR confirmed isolates of *M. gallisepticum* and *M. synoviae* were tested using enrofloxacin, tetracycline, gentamicin, spiroomicin and tylosin.

The isolates of *Mycoplasma gallisepticum* showed a variable degree of resistance against the antibiotics tested, with a significantly high MIC₅₀ of Enrofloxacin as compared to other antibiotics tested followed by tetracycline, gentamicin, spiroomicin and tylosin. This is similar to the findings reported by Behbahan and co-workers (33) and the findings of (16, 34, 36, 37). On the other hand, a previous study of MG isolates from Israel had increased resistance to enrofloxacin (26, 35).

In the case of *Mycoplasma synoviae* (MS), significantly high MIC against enrofloxacin, followed by tetracycline, spiroomicin, tylosin and gentamicin (46.4±2.18 µg/ml). These findings were similar to those of (25, 38, 39).

The results of the current study elucidate the significant losses incurred by poultry birds due to high morbidity and mortality, along with production losses. The multiplex PCR is an efficient, reliable and reproducible tool for the rapid confirmation and diagnosis of avian mycoplasmosis. The severity of the problem is of utmost importance and needs to be further investigated using classical diagnostic methods, along with latest molecular techniques for assessment of the disease scenario. There is a huge need to update the therapeutic regimen owing to increased antibiotic resistance from time to time.

Acknowledgement

This research was supported by Higher Education Commission Pakistan under indigenous scholarship program. We thank David A Morrison for his work on the manuscript in proof correcting.

References

1. OIE. Avian mycoplasmosis (*Mycoplasma gallisepticum*, *M. synoviae*). In: Manual of diagnostic tests and vaccines for terrestrial animals. Paris : Office International des Epizooties, 2008: 482–96.
2. Kleven SH, Ferguson-Noel N. *Mycoplasma synoviae* infection. In: Saif YM, Barnes HJ, Glisson JR, et al., eds. Diseases of poultry. London : Blackwell Publishers, 2008: 845–56.
3. Kleven SH. Control of avian mycoplasma infections in commercial poultry. Avian Dis 2008; 52: 367–74.
4. Luciano RL, Cardoso ALSP, Stoppa GFZ, et

- al. Comparative study of serological tests for *Mycoplasma synoviae* diagnosis in commercial poultry breeders. *Vet Med Int* 2011; 2011: Art 304349. doi: 10.4061/2011/304349
5. Mohana MA, Haider M, Kadhim AH, et al. Molecular diagnosis of avian respiratory diseases in commercial broiler chicken flocks in province of Najaf, Iraq. *Sci Res Essays* 2013; 8: 1191–5.
6. Yashpal SM, Devi PP, Sagar MG. Detection of three avian respiratory viruses by single-tube multiplex reverse transcription-polymerase chain reaction assay. *J Vet Diagn Invest* 2004; 16: 244–8.
7. Gabriel SC, Shivaprasad HL, Chin RP. Systemic *Mycoplasma synoviae* infection in broiler chickens. *Avian Pathol* 2005; 34: 137–42.
8. Ley DH. *Mycoplasma gallisepticum* infection. In: Saif, YM, et al., eds. *Diseases of poultry*. Ames : Iowa State University Press, 2008: 805–33.
9. Jeon EO, Kim JN, Lee HR, et al. Eggshell apex abnormalities associated with *Mycoplasma synoviae* infection in layers. *J Vet Sci* 2014; 15: 579–82.
10. Levisohn S, Kleven SH. Avian mycoplasmosis (*Mycoplasma gallisepticum*). *Rev Sci Tech* 2000; 19: 425–42.
11. Gautier-Bouchardon AV, Reinhardt AK, Kobisch M, Kempf I. In vitro development of resistance to enrofloxacin, erythromycin, tylosin, tiamulin and oxytetracycline in *Mycoplasma gallisepticum*, *Mycoplasma iowae* and *Mycoplasma synoviae*. *Vet Microbiol* 2002; 88: 47–58.
12. Hannan PC, Windsor GD, De Jong A, Schmeer N, Stegemann M. Comparative susceptibilities of various animal-pathogenic mycoplasmas to fluoroquinolones. *Antimicrob Agents Chemother* 1997; 41: 2037–40.
13. Ter Laak EA, Noordergraaf JH, Verschure MH. Susceptibilities of *Mycoplasma bovis*, *Mycoplasma dispar*, and *Ureaplasma diversum* strains to antimicrobial agents in vitro. *Antimicrob Agents Chemother* 1993; 37: 317–21.
14. Bradbury JM, Yavari CA, Giles CJ. In vitro evaluation of various antimicrobials against *Mycoplasma gallisepticum* and *Mycoplasma synoviae* by the micro-broth method, and comparison with a commercially-prepared test system. *Avian Pathol* 1994; 23: 105–15.
15. Hannan PC. Guidelines and recommendations for antimicrobial minimum inhibitory concentration (MIC) testing against veterinary mycoplasma species. *Vet Res* 2000; 31(4): 373–95.
16. Wu CM, Wu H, Ning Y, Wang J, Du X, Shen J. Induction of macrolide resistance in *Mycoplasma gallisepticum* in vitro and its resistance-related mutations with domain V of 23S rRNA. *FEMS Microbiol Lett* 2005; 247: 199–205.
17. Nicholas RAJ, Ayling RD. *Mycoplasma bovis*: disease, diagnosis, and control. *Res Vet Sci* 2003; 74: 105–12.
18. Ahmad A, Khan TA, Kanwal B, et al. Molecular identification of agents causing respiratory infections in chickens from southern region of Pakistan from October 2007 to February 2008. *Int J Agr Biol* 2009; 11: 325–8.
19. Stipkovits L, Kempf I. Mycoplasmosis in poultry. *Rev Sci Tech* 1996; 15: 1495–525.
20. Bencina D, Bradbury JM, Stripkovits L, et al. Isolation of *Mycoplasma capriculum*-like strains from chickens. *Vet Microbiol* 2006; 112(1): 23–31.
21. Jackwood MW, Hilt DA, Williams SM, et al. Molecular and serologic characterization, pathogenicity, and protection studies with infectious bronchitis virus field isolates from California. *Avian Dis* 2007; 51: 527–33.
22. Siddique AB, Rahman SU, Hussain I, et al. Frequency distribution of opportunistic avian pathogens in respiratory distress cases of poultry. *Pak Vet J* 2012; 32: 386–9.
23. Marois C, Gesbert FD, Kempf I. Polymerase chain reaction for the detection of *Mycoplasma gallisepticum* from environmental samples. *Avian Pathol* 2002; 31: 163–8.
24. Wang C, Ewing M, A'arabi SY. *In vitro* susceptibility of avian mycoplasmas to enrofloxacin, sarafloxacin, tylosin, and oxytetracycline. *Avian Dis* 2001; 45: 456–60.
25. Cerda RO, Giacoboni GI, Xavier JA, Sanzalone PI, Landoni MF. *In vitro* antibiotic susceptibility of field isolates of *Mycoplasma synoviae* in Argentina. *Avian Dis* 2002; 46: 215–8.
26. Gerchman I, Lysnyansky I, Perk S, Levisohn S. *In vitro* susceptibilities to fluoroquinolones in current and archived *Mycoplasma gallisepticum* and *Mycoplasma synoviae* isolates from meat-type turkeys. *Vet Microbiol* 2008; 131: 266–76.
27. Ehtisham-ul-Haque S, Rahman SU, Siddique M, Qureshi AS. Involvement of *Mycoplasma synoviae* in respiratory distress cases of broilers. *Pak Vet J* 2011; 31: 117–9.
28. Seifi S, Asasi K, Mohammadi A. Natural co-infection caused by avian influenza H9 subtype and infectious bronchitis viruses in broiler chicken farms. *Vet Arh* 2010; 80: 269–81.

29. Yousaf AM, Aradaib IE, Khairalla KMS, Sbdalla MA, Karrar ARE, ElHusseini ARM. Evaluation of RT-PCR for rapid detection of Sudanese isolates and vaccine strains of Newcastle disease. *Pak J Biol Sci* 2005; 8: 418–20.
30. Wang H, Fadl AA, Khan MI. Multiplex PCR for avian pathogenic mycoplasmas. *Mol Cell Probes* 1997; 11: 211–6.
31. Hong Y, García M, Leiting V, et al. Specific detection and typing of *Mycoplasma synoviae* strains in poultry with PCR and DNA sequence analysis targeting the hemagglutinin encoding gene *vlhA*. *Avian Dis* 2004; 48: 606–16.
32. Harada K, Tanaka MK, Uchiyama M, et al. Molecular typing of Japanese field isolates and live commercial vaccine strain of *Mycoplasma synoviae* using improved pulsed-field gel electrophoresis and *vlhA* gene sequencing. *Avian Dis* 2009; 53(4): 538–43.
33. Behbahan NGG, Asasi K, Afsharifar AR, Pourbakhsh SA. Susceptibilities of *Mycoplasma gallisepticum* and *Mycoplasma synoviae* isolates to antimicrobial agents *in vitro*. *Int J Poult Sci* 2008; 7: 1058–64.
34. Reinhardt AK, Gautier-Bouchardon AV, Gicquel-Bruneau M, Kobisch M, Kempf I. Persistence of *Mycoplasma gallisepticum* in chickens after treatment with enrofloxacin without development of resistance. *Vet Microbiol* 2005; 106(1/2): 129–37.
35. Gharaibeh S, Al-Rashdan M. Change in antimicrobial susceptibility of *Mycoplasma gallisepticum* field isolates. *Vet Microbiol* 2011; 150(3/4): 379–83.
36. Jordan FT, Horrocks BK. The minimum inhibitory concentration of tilmicosin and tylosin for *Mycoplasma gallisepticum* and *Mycoplasma synoviae* and a comparison of their efficacy in the control on *Mycoplasma gallisepticum* infection in broiler chicks. *Avian Dis* 1996; 40: 326–34.
37. Jordan FT, Forrester CA, Ripley PH, Burch DG. *In vitro* and *in vivo* comparison of valnemulin, tiamulin, tylosin, enrofloxacin and lincomycin/spectinomycin against *Mycoplasma gallisepticum*. *Avian Dis* 1998; 42(4): 738–45.
38. Le Carrou J, Reinhardt AK, Kempf I, Gautier-Bouchardon AV. Persistence of *Mycoplasma synoviae* in hens after two enrofloxacin treatments and detection of mutations in the *parC* gene. *Vet Res* 2006; 37(1): 145–54.
39. Senties CG, Shivaprasad HL, Chin RP. Systemic *Mycoplasma synoviae* infection in broiler chickens. *Avian Pathol* 2005; 34: 137–42.
40. Nascimento ER, Pereira VL, Nascimento MG, Barreto ML. Avian mycoplasmosis update. *Braz J Poult Sci* 2005; 7(1): e1. doi: 10.1590/S1516-635X2005000100001
41. Kurska O, Pakuła A, Tomczyk G, et al. Eggshell apex abnormalities caused by two different *Mycoplasma synoviae* genotypes and evaluation of eggshell anomalies by full-field optical coherence tomography. *BMC Vet Res* 2019; 15(1): e1. doi: 10.1186/s12917-018-1758-8

POJAVNOST, MOLEKULARNA IDENTIFIKACIJA IN UGOTAVLJANJE ODPORNOSTI NA ANTIBIOTIKE MIKOBAKTERIJ *MYCOPLASMA GALLISEPTICUM* IN *MYCOPLASMA SYNOVIAE* IZOLIRANIH IZ KOKOŠI S KRONIČNIMI DIHALNIMI BOLENJI IN IZ NJIHOVEGA BIVALNEGA OKOLJA

A. B. Siddique, S. U. Rahman, M. Ulhaq, R. Naveed

Povzetek: Ptičja mikoplazmoza je resno težava v perutninski proizvodnji, ki vodi v velike izgube zaradi obolevanja perutnine in posledično povzroča ekonomske izgube. Glavni povzročitelji mikoplazmoz so *Mycoplasma gallisepticum* in *Mycoplasma synoviae*. Za preučevanje spremenljive stopnje odpornosti na običajno predpisane in uporabljene antibiotike pri mikoplazmozi je bilo odvzetih skupno 115 vzorcev, vključno z vzorci tkiva in brisom, pitovnih piščancev, nesnic s kroničnimi boleznimi dihal (CRD) in iz njihovega bivalnega okolja. Vzorci so bili preneseni v tekoče gojišče BHI (iz angl. Brain Heart Infusion), z dodatkom 10 % konjskega seruma, NAD, cisteina, penicilina in talijevega acetata. Pozitivne vzorce smo prenesli v agar BHI (Difco) za izolacijo *Mycoplasma spp.* Vzorci so bili določeni kot negativni po tretji pasaži. Med vzorci je bilo 61,5 % pozitivnih na prisotnost *Mycoplasma spp.*, ki smo jih večinoma ugotovili po drugi pasaži. Od vseh pozitivnih primerov je bila ugotovljena *Mycoplasma gallisepticum* (MG) v 62 % primerov, *Mycoplasma synoviae* (MS) pa v 38 %, kar je bilo potrjeno z verižno reakcijo s polimerazo (PCR) z uporabo specifičnih primerjev. Izolati MG in MS so pokazali spremenljivo stopnjo občutljivosti na komercialno dostopno zdravilo tilozin. Minimalna zaviralna koncentracija (MIC) pri MG je bila najvišja pri enrofloksacinu ($112,38 \pm 4,34 \mu\text{g/ml}$), sledili pa so tetraciklin ($91,58 \pm 4,66 \mu\text{l/ml}$), gentamicin ($54,33 \pm 2,98 \mu\text{g/ml}$), spiromicin ($52,23 \pm 3,99 \mu\text{g/ml}$) in tilozin ($52,58 \pm 2,69 \mu\text{g/ml}$). Najvišjo MIC proti MS smo ravno takougotovili pri enrofloksacinu ($168,24 \pm 3,82 \mu\text{g/ml}$), ki so mu sledili tetraciklin ($115,48 \pm 2,62 \mu\text{g/ml}$), spiromicin ($95,96 \pm 2,17 \mu\text{g/ml}$), tilozin ($84,84 \pm 2,56 \mu\text{g/ml}$) in gentamicin ($46,4 \pm 2,18 \mu\text{g/ml}$).

Ključne besede: ptičja mikoplazmoza; kronična bolezen dihal; minimalna zaviralna koncentracija; mnogokranta PCR reakcija

COMPARISONS OF THE HISTOLOGICAL MORPHOLOGY AND IN VITRO PERCUTANEOUS ABSORPTION OF CAFFEINE IN SHED SNAKE SKIN AND HUMAN SKIN

Manuel Sacha*, Nancy Weisbach, Anna-Sophie Pöhler, Nina Demmerle, Eleonore Haltner

Across Barriers GmbH, Science Park 1, Saarbrücken, Germany

*Corresponding author, E-mail: m.sacha@acrossbarriers.de

Abstract: The employment of excised skin (human or animal) mounted in diffusion cells is frequently used for the characterization of biopharmaceutical properties of topical semisolids dosage forms. Reptile skin from snake appears to be a useful alternative to other animal and human skins in assessing the potential for transdermal drug delivery. The aim of the study was to compare human and snake skin from a histological point of view. Furthermore the absorption of caffeine, as a hydrophilic model substance, was compared on snake shed skins (two anatomical locations; ventral and dorsal), from three different species, *Python regius*, *Epicrates maurus colombianus*, *Lampropeltis triangulum campbelli*, and human skin. Snake skin shows histological similarity to human *Stratum corneum* in term of thickness and composition. Regarding the absorption, the cumulative amount of caffeine increased linearly with time through the dorsal and ventral shed skins of all 3 species. Except for *Lampropeltis triangulum campbelli* ventral skin, the caffeine permeation behavior obtained on all snake shed skins evaluated was in a similar range as on human skin. One main advantage of shed skin, is that snakes molt regularly and can provide many sheds, that can be obtained without sacrificing the animals.

Key words: caffeine; transdermal; shed skin; *in vitro*; snake; topical formulation

Introduction

Transdermal drug delivery (TDD) is an alternative to gastrointestinal administration systems. The bypassing of the intestinal tract avoids first-pass metabolism, and can reduce the risk of toxicity and increases patient compliance. Pharmaceutical companies are focusing on the elaboration of new topical formulations. For the facilitation and shortening of the generally lengthy and resource consuming pharmaceutical development procedures, *in vitro* models are

becoming increasingly popular (1, 2). Currently the tendency is the decreased interest and acceptance for animal testing (3).

In the last twenty years, the trend of the scientific community was to reduce the number of animals used in preclinical and further scientific experiments. The 3Rs (Replacement, Reduction, Refinement) guiding principle (4) try to be progressively adopted by various research institutes in order to set up animal alternatives testing methods based on cell or tissue *in vitro* assays. This innovative point of view is in accordance with the animal rights. But new *in vitro* models, which correlate as much as possible to human *in vivo* conditions, are still needed. Currently, *in vitro*

Franz diffusion experiments have been recognized as one of the most significant tool to investigate transdermal drug administration.

According to the OECD 428 guideline (5), various excised skins, full or dermatomed, from human or animal origins can be used as biological membrane mounted in Franz diffusion cells to evaluate the absorption of molecules from topical formulations. Skin membranes can be prepared in different manners, but the most important layer, *Stratum corneum* (SC) representing the main barrier of the tissue, must remain intact for the investigations. Physiological buffer is recommended as acceptor medium, in order to simulate the systemic circulation. Samples are drawn at define time intervals or continuously (5).

Excised human skin is considered to be the most predictive membrane for *in vitro* permeation studies. But ethical considerations and scarcity of the tissue represent the main problems for the laboratories to use human skin for percutaneous absorption evaluations. Therefore, animal skins that are histologically similar to human skin, such as porcine skin (sometimes obtained from slaughterhouses), are often used as alternatives, but require sacrificing the animal (5).

Based on lipid composition as well as on thickness of the *Stratum corneum*, snake skin (reptile) appears to be an interesting substitute of human and further animal skins (6).

In 1988 Higuchi and Kans introduced for the first time the concept of using snake shed skin as biological barrier for *in vitro* percutaneous studies (7).

One major benefit of snake shed skin is that the molting process occurs regularly (e.g. once a month), providing therefore multiple sheds from a single individual. The variability between individual as it is the case in other models is excluded (8).

Further non-negligible advantage, is that the skin can be obtained without sacrificing the animals. Also, zoos in each country can make these tissues easily accessible for the laboratories. The tissue is "dead" biological material therefore storable at room temperature.

Here, we present, after a histological comparison between human and reptile skin, the results of *in vitro* permeation testing for snake shed skin compared to human skin using a well-established Franz cell diffusion method and caffeine as marker. Caffeine, a high permeable marker, with

high biological activity properties (degradation of fat, cells protection against UV, stimulation of hair growth (9), is often included in cosmetic formulations. Furthermore this molecule is used as hydrophilic quality control molecule, in *in vivo* as well as *in vitro* absorption studies with human or animal skin (5).

It is not well known on the use of shed snake skin as a substitute for the human skin. For this purpose, shed skins (in two anatomical locations: ventral and dorsal) of three different species from three different families of snakes, Colubridae, Boidae, and Pythonidae, were compared to human skin.

Material and methods

Anhydrous caffeine (purity: 99.9 %, molecular weight: 194.19 g.mol⁻¹, log P: -0.07, pKa: 10.4 at 40°C, solubility: 21.6 mg.L⁻¹ at 25 °C (10) used for the preparation of the test solution and as analytical standard was obtained from Carl Roth GmbH (Karlsruhe, Germany). PBS (phosphate buffered saline) powder without Ca²⁺ and Mg²⁺, was supplied by Biochrom GmbH (Berlin, Germany). Hematoxylin and all further reagents used for Histology were from Dako belonging to Agilent Technologies GmbH (Waldbronn, Germany).

Caffeine solution for topical administration

A caffeine solution with a concentration of approximately 10 mg.mL⁻¹ was prepared. The caffeine was weighed in a volumetric flask and filled up to the mark with PBS-buffer pH 7.4. Finally, the solution was shaken until completely dissolved.

The PBS buffer pH 7.4 without Mg ions and Ca ions was prepared as follows: 9.55 g dry substance (e.g. Dulbecco's phosphate buffered saline from Biochrom) was transferred into a 1 liter volumetric flask and dissolved in 900 mL purified water. The pH value was controlled and adjusted to 7.40 ± 0.05 with ortho-phosphoric acid. Afterwards the flask was filled up with purified water. The solution was degassed in an ultra-sonic bath for at least 15 minutes prior to use. The composition (according to supplier Biochrom) is as follows: 8000 mg/L NaCl; 200 mg/L KCl; 1150 mg/L Na₂HPO₄; 200 mg/L KH₂PO₄.

Permeation across human and snake shed skins

Human skin

This *ex vivo* absorption method was based on the Organisation for Economic Cooperation and Development (OECD) Test No. 428: Skin absorption: *in vitro* method (OECD, 2004) (5). Human abdominal skin samples from twenty three patients were obtained via surgical skin removal procedures (Dr. Pierre Sibille, reconstructive and cosmetic surgeon, Nancy, France) that were unrelated to the present investigation. Each of the twenty three patients consented to the scientific use of skin prior to surgery. Skin was not used if there was a pathologic finding, skin damage, strongly marked scarring, or pregnancy stretch marks.

The excised skin was cooled to 4°C. Then, the subcutaneous fatty layer was separated from the skin, and the skin specimen was stored at -20°C until use (less than 466 days according to the

OECD guideline 428). To prepare the skin sample for use, the specimen was thawed and cut into strips with a scalpel and dermatomed to a mean thickness of 500±100 µm, leaving the *Stratum corneum* intact.

Snake shed skin

The shed skins of three snake species from three different snake families were obtained after molting from the author's private collection (Figure 1). The three selected species were: from the Colubridae family, *Lampropeltis triangulum campbelli* (Lampropeltis), from the Boidae family, *Epicrates maurus colombianus* (Boa) and *Python regius* (Python) from the Pythonidae family. The tissues were not older than 2 months and stored at room temperature, under dry conditions, until preparation. Humidity condition was not controlled.

The skins were cut to size and hydrated by allowing them to soak overnight in distilled water in a covered petri dish (Figure 2) (11).

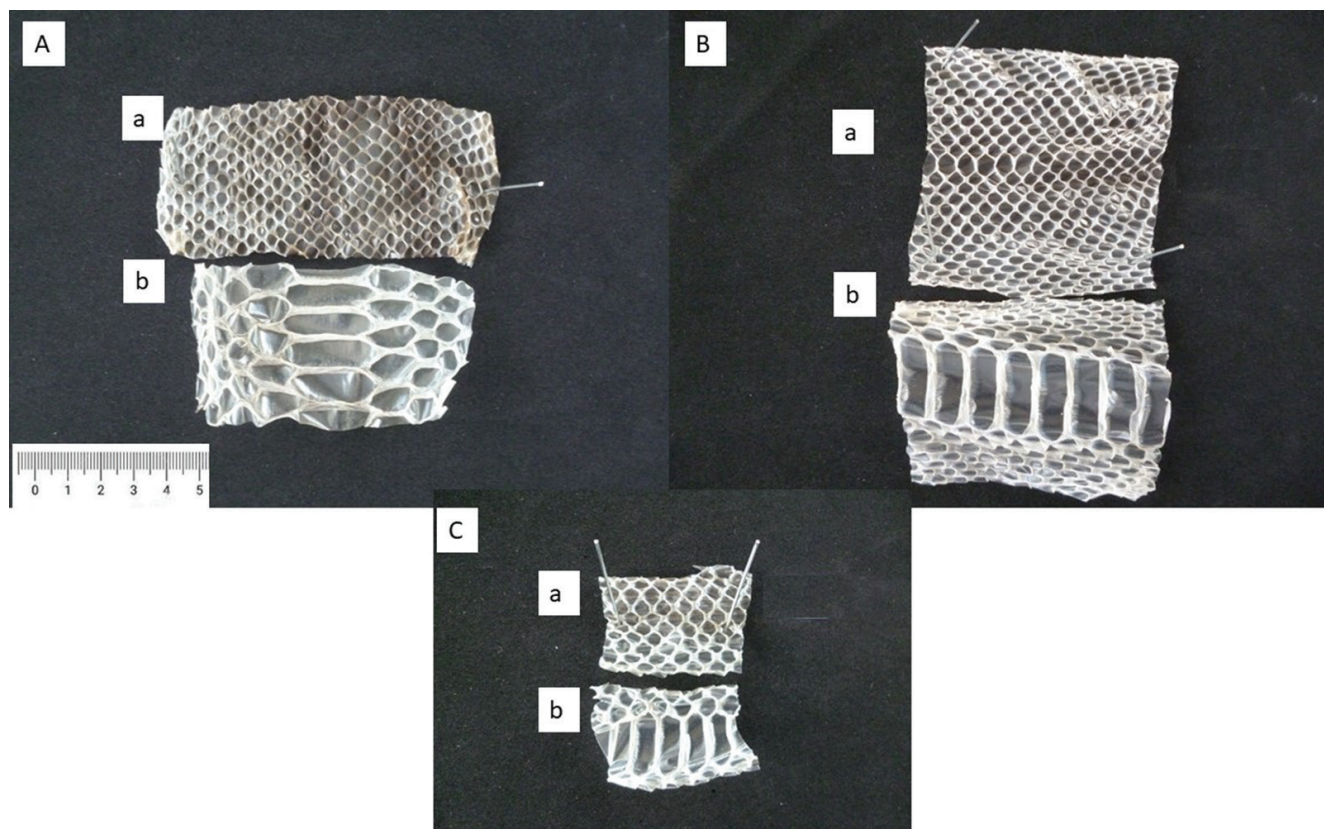


Figure 1: Photographs of the shed snake skins. A. *Python regius*, B. *Epicrates maurus colombianus* and C. *Lampropeltis triangulum campbelli*. a. Dorsal part, b. Ventral part

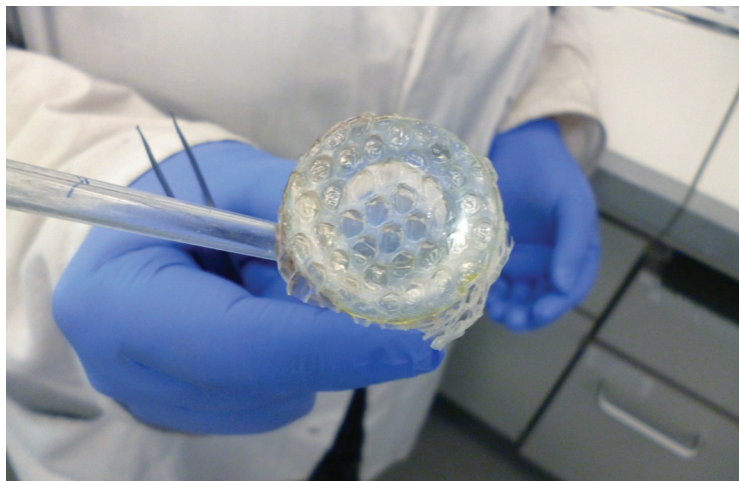


Figure 2: dorsal Python shed snake skin applied on the franz diffusion cell after overnight hydration

Franz cell

Circular samples from each skin specimen were prepared with a hollow punch and placed between the donor and receiver sections of a Franz cell (diffusion area 1.8 cm²), with the *Stratum corneum* facing the donor cell. The receptor compartment medium was PBS pH 7.4 without Mg or Ca ions and was kept at 32±1°C. The receptor compartment was mixed with a magnetic stir bar at 400 rpm.

1.2 ml caffeine solution (10 mg·mL⁻¹) was applied to the skin surface in the donor cell and 320 µL samples were withdrawn from the receiver compartment at 4, 6, 8, 20, 24, 28, 32, 46, and 48 hours. The sampled volume was replaced with phosphate-buffered saline (PBS) after each sample was removed.

Each experiment was done in four fold per skin species.

Analytical methods

Caffeine concentrations were determined using an HPLC (high performance liquid chromatography) serie 1200 from Agilent Technologies GmbH (Waldbronn, Germany) and a 996 PDA (Photo Diode Array) detector from Waters GmbH (Eschborn, Germany). The lower limit of quantification of caffeine was 0.050 µg·mL⁻¹. The column used was a Waters Symmetry C18, 3.5 µm, 4.6 x 75 mm, supplied by Waters GmbH (Eschborn, Germany), set at 40°C. The mobile phases were phosphate buffer pH 3.50 (± 0.05) and acetonitrile run in gradient condition at a flow rate of 1.0 ml·min⁻¹ (gradient profile: 0.0 min; buffer/ACN 90/10 => 2.5 min: buffer/ACN

90/10 => 5.0 min: buffer/ACN 40/60 => 6.0 min: buffer/ACN 40/60 => 6.1 min: buffer/ACN 90/10 => 10.0 min: buffer/ACN 90/10), and detection at 272 nm. The retention time was 3.7 minutes.

Calculations

Apparent permeation coefficient was calculated using Eq. 1:

$$P_{app} = \frac{dQ}{dt} \cdot \frac{1}{m_0} \cdot \frac{1}{A} \cdot V_D \quad (1)$$

P_{app} is the apparent permeation coefficient (cm·s⁻¹)
 dQ/dt is the steady state transport rate obtained by linear regression of the amount of test substance transported vs time (µg·s⁻¹)
 m_0 is the initial mass of test substance in the donor compartment (µg)
 A is the area of exposed skin (cm²)
 and V_D is the donor volume (cm³)

Statistical methods

Differences in cumulative transport through the skin samples were compared with a non-parametric Mann-Whitney U- test. All results are expressed as mean ± standard deviation.

Histology

Human and reptile skin tissues (not thicker than 3 mm) were fixed in 10 % formalin at room temperature for 8 hours and then dehydrated in a grade series of ethanol baths (70 % ethanol for 1 hour, 95 % ethanol for 1 hour twice, 100 %

ethanol for 1 hour twice). The tissue was cleared in xylene for 1 hour (2 times), then embedded in paraffin blocks. Paraffin sections were done at a thickness of 4 to 5 μm from paraffin blocks. The obtained slides were allowed to dry overnight. The next day the slides were placed in a 55 °C oven for ten minutes to melt the paraffin. Deparaffinize was done by using two changes of Xylene for 5 minutes, two changes of 100 % alcohol and 95 % alcohol for 3 minutes each. The staining was performed by using hematoxylin. The mounted slides were examined using a Leica DM4000 B Microscope, and photographed by a Leica MC120HD HD Camera from Leica Mikrosysteme Vertrieb GmbH (Wetzlar, Germany).

Results

Histology

Like mammalian skin, reptile skin consists of two main layers: the epidermis at the surface and the dermis underneath.

Reptile epidermis (see figure 3 A) is characterized by the presence of a unique thick, horny surface featured with epidermal scales. Integumentary glands are not abundant. Snake shed skin and human *Stratum corneum* present analogies. The tissue thickness is similar with 13-15 μm and 10–20 μm in respectively human and snake shed skin. The structure for keratin type α and β (β : only reptiles and birds) as well as the lipid composition is comparable in both tissues (2.0–6.5% in human

Stratum corneum and 6.0% in snake shed skin) (12).

The main difference is that human epidermis has a dense *Stratum corneum* (see figure 3 B), with hairs present arising from hair follicles. In addition, in human skin, epidermal glands including sebaceous or sudoriferous glands are present.

Reptile epidermis is composed of three cell layers arranged from the bottom to the surface as follows (see figure 4A):

Stratum germinativum or basal layer composed of undifferentiated growing cells ensuring the renewal of the epidermis

Stratum intermedium or intermediate zone composed of cells in migration and producing keratin. The cells become flatter as they reach the surface.

Stratum corneum, the third layer of the epidermis, is constituted of three layers: an α keratin layer, a β keratin layer and the third layer named Oberhäutchen (13). These layers are composed of highly keratinized flat dead cells. α keratin is similar to the keratin in the composition of the hair in mammals. β keratin is similar to the keratin in the composition of bird feather. These two layers provide flexibility to the epidermis, due to the α keratin helical structure, but also inflexibility, due to the β keratin pleated sheet structure. The β keratin is predominant on the outer scale surface (providing the rigidity to ensure the protection function of the skin) and is attenuated on the inner scale surface and hinge region. In the hinge region of the scales, α keratin is more present, providing the elasticity to this area. The epidermis of the belly

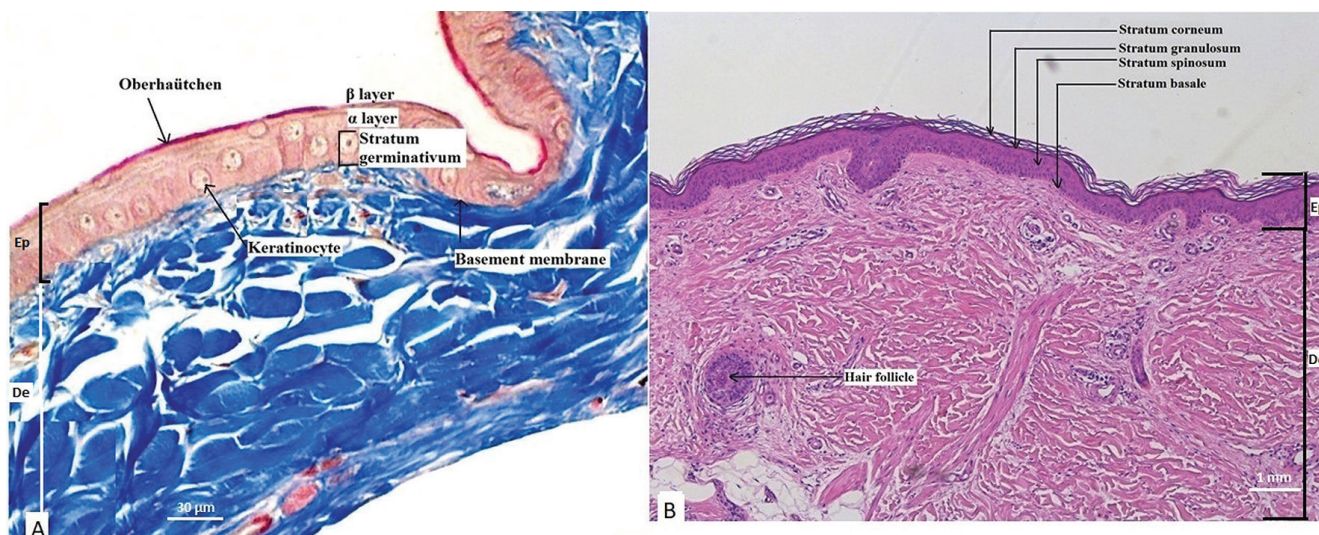


Figure 3: Photomicrograph of histological sections of reptile and human skins. A. reptile dorsal skin X400. B. human skin, X5. *Stratum lucidum* is not visible. Ep: Epidermis, De: Dermis

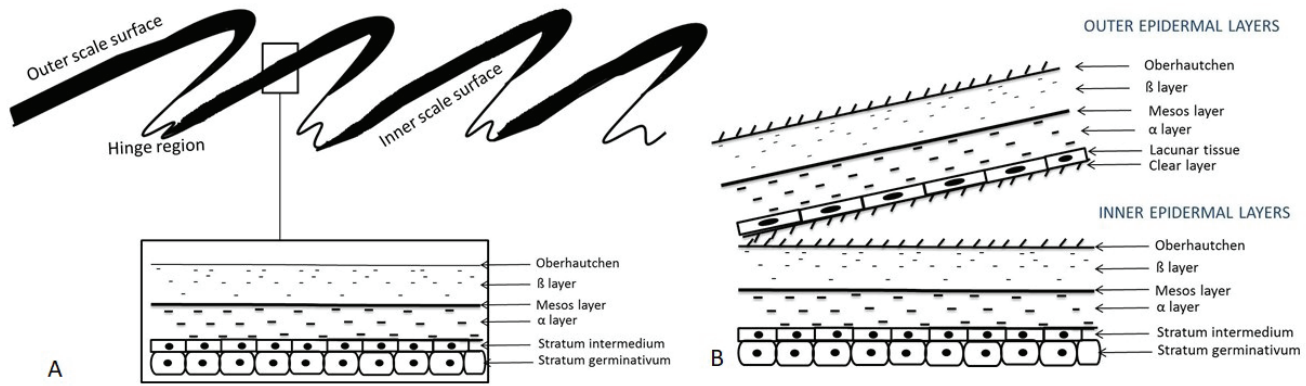


Figure 4: Diagrammatic representations of snake skin. A. transverse section of snake skin (adapted from Roberts 1986) (14). B. Terminal differentiation in the shedding cycle stage 5 and 6

is composed of a thicker and keratin rich layer to insure the protection against roughness of the ground or other substrate. Between these keratin layers (α and β) appears a polar lipid layer (named mesos layer), which plays a role in the permeability of the skin to water, gases, and other molecules.

The dermis located below the epidermis is at least four times as thick, and consists of a connective tissue containing abundant collagen fibers arranged in a reticular pattern, as well as blood vessels, sensorial receptors, and nerves. The main difference compared to mammalian skin is the lack of glands, follicular hairs, and arrector muscles. The hypodermis is mainly composed of a layer of abundant subcutaneous adipose tissue and overlies a deep fascia and skeletal muscle fibers.

Physiological molting (Ecdysis)

Molting can be a continuous renewal as seen in mammalian epidermis. This mode is adopted by most chelonians and crocodilians. The other mode is the episodic shedding of epidermis, as adopted by squamate reptiles.

Molting is a physiological mechanism dependent on the thyroid hormones. These hormones are able to stimulate the molting process in saurians, while they inhibit the process in ophidians.

The sloughing cycle of the multilayered epidermis can be divided into two phases: resting phase and renewal phase (15).

The resting phase is represented by stage 1. It starts after the molt of the animal, and can be further divided into immediate post-shedding phase, the perfect resting phase and the prerenewal phase or late resting phase. The duration varies from a couple of days to months.

The renewal phase goes from stage 2 to stage 6.

The stage 2 is characterized by an important multiplication of cells in the *Stratum germinativum*. The process leads to the formation of an intra-epidermal shedding layer. The skin becomes dull. The beginning of the renewal phase takes about 5-7 days.

In the stage 3, the new generated cells undergo a differentiation/keratinization process. Two pathways are used, α and β , leading to cells containing, respectively, α and β keratin. The skin appears very dull and snake eyes are opaque. The duration of this phase is about 3-4 days.

The stage 4 is defined by the production of a new epidermis. The layers of this outer epidermis are constituted of cells, differentiated and keratinized, distributed in an outer *Oberhäutchen*, β layer, mesos layer, α layer, lacunar tissue, and a clear layer. The remaining inner epidermal layers consists of an inner *Oberhäutchen*, inner β layer, inner mesos layer, as well as a non completed α and basal layer. This step takes about 5 to 10 days.

In the stage 5 (see figure 4B), the area between the 2 generations of epidermis (outer epidermal generation and inner epidermal generation) will be filled by lymph and enzymes. The skin and eyes become clear and shiny. The shedding of the old epidermis begins 3-4 days after skin becomes clear.

The stage 6 is the ultimate step of the ecdysis process, consisting of the separation of the outer epidermis or old *Stratum corneum* from the cleavage area. The two generations of epidermis will be separated. After the shedding, the skin becomes harder.

Ex vivo transport of caffeine through snake shed and human skins

Figure 5 presents the cumulative caffeine transport over time on each snake shed skin. The cumulative amount of caffeine increased linearly with time through the dorsal and ventral shed skin of all 3 species, corresponding to a typical passive diffusion. After 48 hours, the cumulative amount of caffeine transported across the Lampropeltis dorsal skin was about twice the

amount transported across Boa dorsal skin, and about 3.5 times higher than the amount across Python dorsal skin (see table 1).

The most permeable was the Lampropeltis skin, with ventral as permeable as dorsal (no statistical difference, $p > 0.05$). Boa skin displayed intermediate permeability with ventral skin more permeable than dorsal (statistically different, $p < 0.05$). Python skin was the least permeable with dorsal and ventral skin producing identical results.

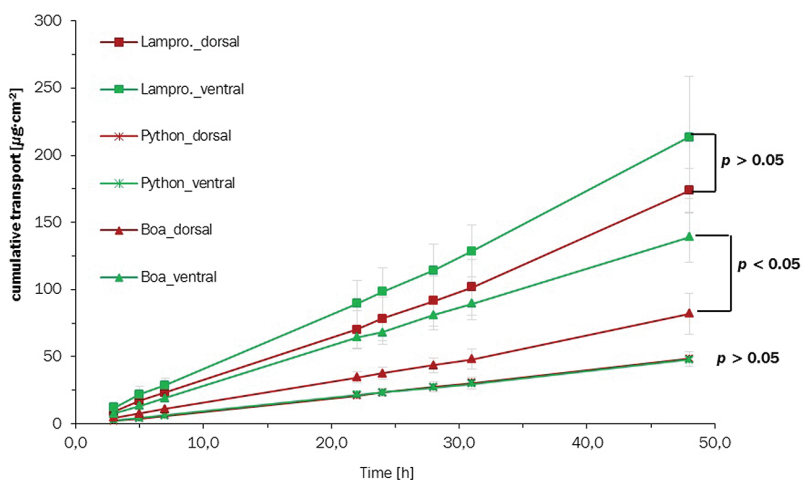


Figure 5: *Ex vivo* percutaneous transport of Caffeine through shed skins. The cumulative transport ($\mu\text{g}\cdot\text{cm}^{-2}$) was calculated by the caffeine concentration determined by HPLC at each sampling time point from the receptor medium. The experiments were performed in four-fold for each skin (ventral and dorsal shed skin of the 3 snake species). Data are shown as mean values of the 4 determinations

Table 1: Cumulative transport of caffeine after 48 hours, and Papp values on snake shed skins samples *ex vivo*. Values are presented as mean \pm SD

Membrane	Cumulative transport after 48 hours ($\mu\text{g}\cdot\text{cm}^{-2}$)	SD ($\mu\text{g}\cdot\text{cm}^{-2}$)	Papp values (cm/s)	SD (cm/s)	RSD (%)
Lampropeltis dorsal	173.71	16.73	8.91E-08	1.76E-08	19.75
Lampropeltis ventral	213.44	45.39	1.23E-07	2.62E-08	21.26
Python dorsal	48.36	5.26	2.79E-08	3.04E-09	10.87
Python ventral	47.73	1.13	2.76E-08	6.56E-10	2.38
Boa dorsal	82.08	15.37	4.75E-08	9.89E-09	20.79
Boa ventral	138.95	18.41	8.05E-08	1.07E-08	13.25

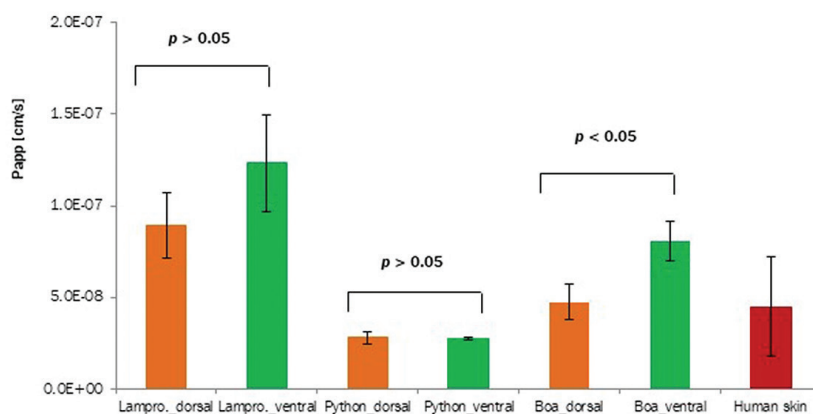


Figure 6: Analyses of apparent permeability rate of caffeine transported in acceptor compartment (Papp) through a normalized surface of shed skin (dorsal and ventral parts) of the 3 snake species, and human skin. The mean Papp values of 4 determinations are represented ($\text{cm}\cdot\text{s}^{-1}$). Statistically significant differences are shown by brackets (Mann-Whitney U test)

Table 2: Comparison of apparent permeability coefficients for caffeine through 23 different dermatomized skin specimens with intact SC. In bold are the snake shed skins

Skin number	Mean P_{app} [$\text{cm}\cdot\text{s}^{-1}$]	SD [$\text{cm}\cdot\text{s}^{-1}$]	RSD [%]
0897-01-1017	1.31E-08	9.17E-10	7.00
557-01-1113	1.45E-08	4.93E-09	34.00
0880-01-0717	1.73E-08	3.11E-09	18.00
0878-01-0717	1.76E-08	3.17E-09	18.00
0722-01-1015	1.93E-08	4.05E-09	21.00
559-01-1213	2.04E-08	1.63E-09	8.00
0875-01-0617	2.18E-08	6.54E-09	30.00
0901-01-1117	2.38E-08	3.81E-09	16.00
150-01-1203	2.54E-08	1.42E-08	56.00
Python ventral	2.76E-08	4.86E-09	2.38
Python dorsal	2.79E-08	6.18E-09	10.87
0724-01-1015	3.04E-08	7.58E-09	16.00
0898-01-1117	3.25E-08	6.99E-09	19.00
0737-01-1115	3.99E-08	1.04E-08	19.00
0747-01-0116	4.11E-08	9.61E-09	17.00
537-01-1013	4.17E-08	3.38E-09	25.00
Boa dorsal	4.75E-08	2.32E-08	20.79
062-01-0701	5.34E-08	2.12E-08	18.00
060-01-0601	5.63E-08	3.21E-08	6.00
0826-01-1116	5.96E-08	2.50E-08	39.00
0768-01-0416	6.42E-08	2.35E-08	33.00
Boa ventral	8.05E-08	2.15E-08	13.25
059-01-0601	8.24E-08	2.84E-08	39.00
0728-01-1115	8.34E-08	9.17E-10	30.00
153-01-0104	8.41E-08	4.93E-09	28.00
Lamprop. dorsal	8.91E-08	3.11E-09	19.75
0887-01-0917	9.35E-08	3.17E-09	23.00
061-01-0701	9.78E-08	4.05E-09	29.00
Lampropeltis ventral	1.23E-07	1.63E-09	21.26

The mean permeation coefficient (mean P_{app}), was derived from slope of the linear portion of the cumulative transport curves (see figure 6, table 1).

Table 2 provides an overview of caffeine permeability through 23 human dermatomed skin specimens, including the P_{app} values obtained with the snake shed skins

All the P_{app} values on shed skins are within the same magnitude compared with data obtained on human dermatomed skins from 23 different donors under the same conditions using the same methods (see table 2).

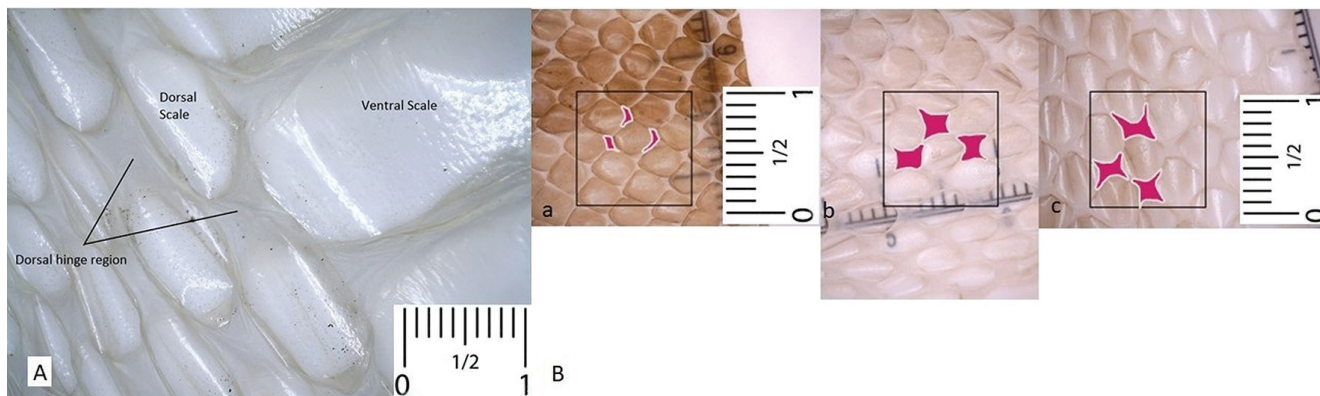


Figure 7: Photographs of scales and hinge areas of not hydrated shed snake skins. A. dorsal and ventral scales, and hinge areas of *Boa* (*Epicrates maurus colombianus*). B. dorsal shed skin of the 3 snake species. a. *Python regius*, b. *Epicrates maurus colombianus*, c. *Lampropeltis triangulum campbelli*. Red color indicates the hinge area. Scales refer to 1 centimeter

Discussion

The difference in permeability of caffeine between the snake shed skins is difficult to explain. The difference in size and shape of the scales, particularly in the available hinge region, may be a factor. The hinge region, which is constituted mainly of a keratin, provides the elasticity of this area. Furthermore, the region is always considerably thinner than the scale regions composed of a thicker and (β) keratin rich layer (see figures 4A and 7A). Hinge areas are therefore considered to be more permeable. In the *Lampropeltis* and *Boa* dorsal skins, these regions are much larger than in *Python* (see figure 7B). Thus, more caffeine formulation is in contact with these areas, explaining the difference in permeability.

The mean human skin P_{app} values range from $1.31E-08$ to $9.38E-08$ $\text{cm}\cdot\text{s}^{-1}$. The variation observed can be largely attributed to natural human variability in dermal absorption. Except for *Lampropeltis* ventral skin, the caffeine permeation behavior was similar between snake shed skins tested and human skin ($p = 0.594$ and $p = 0.531$ with respectively python dorsal and ventral, $p = 0.762$, and $p = 0.060$ with respectively *Boa* dorsal and *Boa* ventral). Shed skins from one specimen of each snake species were used for the experiments, and therefore the lack of variability may be an explanation for the difference observed with *Lampropeltis* ventral skin.

Even if the snake shed skin only consisted of a part of epidermis (only *Stratum corneum*), in comparison to human dermatomed skin, which contains the complete epidermis and a part of the

dermis, the results show that *Stratum corneum* functions as the main barrier and is sufficient to investigate permeation of markers. Furthermore, at this thickness, the resistance of the dermis, present in dermatomed human skin, to overall skin permeation can be ignored (16) (e.g. Papp value of Caffeine through human epidermis sheets is $6.00 E-08 \pm 0.04$ $\text{cm}\cdot\text{s}^{-1}$ (17).

Ngawhirunpat (2006) (6) compared the *in vitro* percutaneous absorption of hydrophilic molecules using shed snake skin of *Pantherophis obsoletus* and human skin. In shed snake skin, the absorption rates of hydrophilic molecules were until six times lower than in human skin. Ngawhirunpat concluded that the shed snake skin contained significantly less water than human *Stratum corneum*. Therefore, the lower permeability observed in shed snake skin for hydrophilic molecules might be caused by a lower size and/or number of pores in skin layers. But according to Torri (2014) (18), based on the analyses of shed skins from four snake species, depending of their taxon and ecology, the snakes have developed species-specific layers of lipids with different structures and composition for the regulation of water permeability. Therefore, in snake skin, the water absorption changes among species living in different climates and habitats. This may explain a difference of permeability for hydrophilic molecules among the snake skins. The results obtained by Ngawhirunpat on *Pantherophis obsoletus* cannot be generalized, and therefore, cannot automatically be transposed to other snake species. The specific lipid structures in the snakes from predominantly dryland habitats such as *Python regius* can protect

the snake from water lost at high temperatures, and may explain the difference seen in lowest absorption of caffeine in comparison to *Epicrates maurus colombianus*, which come from a wetland/rainforest habitat and have a skin that is more permeable to hydrophilic molecules.

Our results with shed skins from *Python regius*, *Lampropeltis triangulum campbelli*, *Epicrates maurus colombianus*, are in non-correspondence to Ngawhirunpat's findings, when using caffeine as hydrophilic drug, which displays similar percutaneous absorption behavior on human skin. Therefore, depending of the snake species of skin used, and their habitat (desertic, rainforest, etc.) the permeability behavior of hydrophilic drug can be different or similar to human skin.

In addition, Klein (2012) (19) confirmed that the epidermis architecture and material properties of the snake skin may change in relation to the snakes' habitats. Particularly important are the differences observed in the structure of the mesos layer between the species, which play a role in the permeability of the skin to water, gases, and molecules including caffeine.

Conclusion

All three species of snake shed skins displayed different characteristics as caffeine diffusion membranes. The possible variability among snake species may be due to differences observed in skin composition. Except for the ventral skin of *Lampropeltis triangulum campbelli*, the caffeine permeation obtained with all snake shed skins investigated was similar to that of human skin. Snake shed skin seems to be an interesting tool to simulate human skin for studies investigating *in vitro* percutaneous absorption of caffeine. It may help to select the best candidate from several newly developed cosmetic formulations containing this active pharmaceutical ingredient.

Additional hydrophilic and lipophilic molecules should be investigated to validate the snake shed model. More snake species as well as the inter-individual variability must be evaluated.

For future testing of molecules, the main challenge will be to select the most appropriate species of snake whose skin resembles human skin.

Acknowledgements

This study was supported by Dr. Hyun Ik Kim (New Jersey), who provided a full review of the manuscript. Histological works were performed by Kai Emrich from Institut für Pathologie Saarbrücken-Rastpfuhl (Germany). Thanks to Professor Ahmed Aly Ahmed Allam Zoology Department, Faculty of science, Beni-Suef University, Beni-Suef 62511, Egypt, for providing the picture of histological section of reptile dorsal skin

References

1. Tsang VL, Bhatia SN. Three dimensional tissue fabrication. *Adv Drug Deliv Rev* 2004; 56(11): 1635–47. doi:10.1016/j.addr.2004.05.001
2. Kim JB. Three-dimensional *in vitro* tissue culture models of breast cancer—a review. *Breast Cancer Res Treat* 2004; 85(3): 281–91. doi:10.1023/B:BREA.0000025418.88785.2b
3. Kolar R. Animal experimentation. *Sci Eng Ethics* 2006; 12(1): 111–22. doi:10.1007/s11948-006-0011-1
4. EMA Guideline on the principles of regulatory acceptance of 3Rs (replacement, reduction, refinement) testing approaches. EMA/CHMP/CVMP/JEG-3Rs/450091/2012. London : European Medicines Agency, 2016. https://www.ema.europa.eu/en/documents/scientific-guideline/guideline-principles-regulatory-acceptance-3rs-replacement-reduction-refinement-testing-approaches_en (25. Sept. 2019)
5. OECD. Test no. 428: Skin absorption: *In vitro* method. In: Guidelines for the testing of chemicals, Section 4: Health effects. Paris : OECD Publishing, 2004. doi:10.1787/9789264071087-en (9. July 2018)
6. Ngawhirunpat T, Panomsuk S, Opanasopit P, Rojanarata T, Hatanaka T. Comparison of the percutaneous absorption of hydrophilic and lipophilic compounds in shed snake skin and human skin. *Pharmazie* 2006; 61(4): 331–5.
7. Higuchi T, Kans L. Method for *in vitro* determination of transdermal absorption: [patent number US4771004, Sept 13, 1988].
8. Haigh JM, Beyssac E, Chanet L, Aiache JM. *In vitro* permeation of progesterone from a gel through the shed skin of three different snake species. *Int J Pharm* 1998; 170(2): 151–6. doi:10.1016/S0378-5173(98)00064-7

9. Herman A, Herman AP. Caffeine's mechanisms of action and its cosmetic use. *Skin Pharmacol Physiol* 2013; 26: 8–14. doi:10.1159/000343174
10. Caffeine. In: DrugBank. Ottawa : Canadian Institutes of Health Research. <https://www.drugbank.ca/drugs/DB00201> (10. Jan. 2020)
11. Balamurugan M, Weli MA, Edwards G, Al-Harisi A, Al-Kharusi Z. *In vitro* permeation studies of commercially available diclofenac sodium gel (sample analysis using LC-MS/MS) through the two different shed snake skins obtained from various regions of sultanate of Oman: a pilot study. *Latin Am J Pharm* 2013; 32 (7): 1069–73.
12. Rigg PC, Barry BW. Shed snake skin and hairless mouse skin as a model membrane for human skin during permeation studies. *J Invest Dermatol* Baltimore 1990; 94(2): 235–40. doi:10.1111/1523-1747.ep12874561
13. Mader DR. Reptile medicine and surgery. 2nd ed.. St. Louis : Saunders, 2006: 1242 p.
14. Roberts JB. Use of squamate epidermis in percutaneous absorption studies: a review. *J Toxicol Cutaneous Ocul Toxicol* 1986; 5(4): 319–24. doi:10.3109/15569528609036305
15. Chang C, Wu P, Baker U, Maini PK, Alibardi L, Cheng-Ming C. Reptile scale paradigm: Evo-Devo pattern formation and regeneration. *Int J Dev Biol* 2009; 53: 813–26. doi:10.1387/ijdb.072556cc
16. Hatanaka T, Inuma M, Sugibayashi K, Morimoto Y. Prediction of skin permeability of drugs I: Comparison with artificial membrane. *Chem Pharm Bull* 1990; 38: 3452–9. <http://doi.org/10.1248/cpb.38.3452>
17. Schäfer-Korting M, Bock U, Gamer A, et al. Reconstructed human epidermis for skin absorption testing: results of the German prevalidation study. *ATLA* 2006; 34: 283–94. doi:10.1177/026119290603400312
18. Torri C, Mangoni A, Teta R, et al. Skin lipid structure controls water permeability in snake molts. *J Struct Biol* 2014; 185: 99–106. doi:org/10.1016/j.jsb.2013.10.007
19. Klein MCG, Gorb SN. Epidermis architecture and material properties of the skin of four snake species. *J R Soc Interface* 2012; 9: 3140–55. doi:10.1098/rsif.2012.0479

PRIMERJAVA HISTOLOŠKE ZGRADBE TER PERKUTANE ABSORPCIJE KOFEINA IN VITRO V LEVKU KAČ IN ČLOVEŠKI KOŽI

M. Sacha, N. Weisbach, A.S. Pöhler, N. Demmerle, E. Haltner

Povzetek: Koža (človeškega ali živalskega izvora) se pogosto uporablja kot orodje za proučevanje biofarmaceutskih lastnosti topikalnih zdravil. Koža kač bi lahko bila uporabna alternativa drugim živalskim kožam in človeški koži pri oceni sposobnosti prenosa zdravil preko kože. Cilj študije je bil histološka primerjava človeške in kačje kože ter primerjava absorpcije kofeina kot hidrofilne modelne snovi na levkih kač iz dorzalnega in ventralnega področja treh različnih vrst kač: kraljevega pitona (*Python regius*), mavričnega udava (*Epicrates maurus colombianus*), mlečne kače (*Lampropeltis triangulum campbelli*). Kačja koža je histološko podobna človeški glede debeline in sestave roženi plasti (*stratum corneum*). Glavna prednost levitve kač je, da se dogaja večkrat, kar omogoča pridobitev več levkov, ki se jih lahko pridobi brez žrtvovanja živali. Rezultati so pokazali, da se je skupna količina kofeina sčasoma linearno povečevala v dorzalnih in ventralnih levkih pri vseh treh vrstah kač, razen na na ventralnem področju levka mlečne kače (*Lampropeltis triangulum campbelli*), pri katerem je bila prehodnost kofeina podobna kot pri prehodu skozi človeško kožo.

Ključne besede: kofein; transdermalno; levke; *in vitro*; kača; topikalni pripravek

EFFICACY OF AMOXICILLIN (ATCOMOX®) AND/OR ALLICIN ON PERFORMANCE, HAEMATOLOGICAL, BIOCHEMICAL, AND HISTOPATHOLOGICAL CHANGES IN *CLOSTRIDIUM PERFRINGENS* INFECTED CHICKENS

Mohamed Aboubakr^{1*}, Ashraf Elkomy¹, Soad Belih², Mohamed Morad¹, Hassan Shaheen³, Mohamed M. Abdel-Daim^{4,5}

¹Pharmacology Department, Faculty of Veterinary Medicine, Benha University, 13736, Moshtohor, Toukh, Qalioubeya, ²Clinical Pathology Department, Animal Health Research Institute, Tanta Branch, ³ATCO PHARMA For Pharmaceutical Industry, Industrial Quisna Zone, El Menofia, Egypt, ⁴Department of Zoology, College of Science, King Saud University, P.O. Box 2455, Riyadh 11451, Saudi Arabia, ⁵Pharmacology Department, Faculty of Veterinary Medicine, Suez Canal University, Ismailia 41522, Egypt

*Corresponding author, E-mail: mohamed.aboubakr@fvtn.bu.edu.eg

Abstract: The efficacy of amoxicillin and/or allicin in healthy and experimentally *Clostridium perfringens*-infected broiler chickens was investigated. The chicks were equally divided into six groups, and all medications were orally administered via drinking water for five consecutive days: Group 1: non-infected and non-treated; Group 2: infected and non-treated; Group 3: infected and amoxicillin-treated (20 mg/kg b.wt); Group 4: infected and allicin-treated (25 mg/kg b.wt); Group 5: infected and treated with amoxicillin (20 mg/kg b.wt) and allicin (25 mg/kg b.wt); Group 6: infected and treated with amoxicillin (10 mg/kg b.wt) and allicin (25 mg/kg b.wt). Growth performance, haematological and biochemical parameters were recorded. Significant decreases in total protein, albumin, RBCs, Hb, and PCV and a considerable increase in WBCs, AST, ALT, ALP, creatinine, and uric acid in infected chickens were observed. Administration of amoxicillin and/or allicin for treatment of *Clostridium perfringens* infection resulted in improvement in haematological and biochemical changes following infection. A dose of amoxicillin (10 mg) and allicin (25 mg)/kg bwt for treatment of *Clostridium perfringens* infection in broiler chickens is recommended due to its great synergistic effect, reduced mortality, greater safety, and increased economic potential.

Key words: amoxicillin; allicin; efficacy; broilers; biochemical; hematological

Introduction

Necrotic enteritis (NE) is a serious problem in the modern poultry industry (1). It causes reduced growth performance, increased feed costs, decreased absorption and digestion, reduced weight gain, and increased feed conversion ratio due to damage in the intestinal mucosa (2). *Clostridium perfringens* is a gram-positive, anaerobic, spore-forming bacterium found in the gastrointestinal tract of poultry and can be isolated from faeces, dust, feed, and litter (3).

Antimicrobial therapy for bacterial infection is important for reducing massive losses in the poultry industry (4). NE is prevented by using antimicrobials such as amoxicillin, which is one of the most effective β lactam antibiotics (5). Good absorption, penetration into tissues, and broad-spectrum of antimicrobial activity make amoxicillin very useful in veterinary medicine (6). It inhibits the biosynthesis of cell wall mucopeptides during bacterial multiplication and has bactericidal action (7).

Alliin is an organosulfur compound present in garlic, a species of the family Alliaceae (8). Numerous phytochemicals, including alliin could interfere with the formation of phospholipid layers

of the cell wall (9). Consequently, bacteria cannot grow in the presence of allicin (10). It has been shown that garlic enhances the broiler chicken's growth and feed conversion as a natural feed additive (11).

The use of antibiotics as growth promoters is becoming a serious problem. There are some important factors that restrict the use of antibiotics, such as the drug resistance in bacteria and presence of drug residues in meat. To combat the poor performance and the increased susceptibility to diseases resulting from the removal of the antibiotics from the poultry diets, alternatives are sought. The utilisation of growth promoters of natural origin has therefore attracted much interest in recent years (12).

Allicin has a distinctively pungent smell and exhibits antibacterial, antifungal, anti-inflammatory, and antioxidant properties (13). The mechanism of the antioxidant or anti-stress activity of allicin, such as trapping free radicals, have been reported (14). When allicin decomposes, it forms 2-propene sulfenic acid, and this compound binds to the free-radicals. Allicin was reported to reduce cholesterol in the serum and liver (15), inhibit bacterial growth (16) and reduce oxidative stress (12). Allicin also has immuno-stimulatory effect (17).

The present study was carried out to evaluate the efficacy of amoxicillin and/or allicin treatment in broilers experimentally infected with *Clostridium perfringens*, and to evaluate the advantages and possible side effects of such treatment.

Materials and methods

Drugs

Amoxicillin (Atcomox 40%)[®] is an antibiotic manufactured by ATCO Pharma Co, Egypt, as oral soluble powder. The recommended dose is 20 mg/kg b.wt (18). Allicin is an organosulfur compound extracted from the garlic and obtained from the Technofeed Company, USA. The recommended dose is 25 mg/kg b.wt (19).

Experimental chicks:

One-hundred-and-eighty apparently healthy, one-day-old unsexed Hubbard broiler chicks were obtained from the El-Kahera poultry company, in Egypt. Chicks were divided into six groups (each

of 30 chicks). Each group was subdivided into five replicates with six chicks each. Chicks were housed on the floor in separate units following strict hygienic regime. The starting temperature of 32°C was reduced by 2°C each week. Continuous lightning was used; feed and water were provided *ad-libitum* and fed free from any medications balanced commercial ration. Chicks were vaccinated on the 7th day of age against New Castle disease with the HitchnerB₁ vaccine and against Gumboro disease at 14 days of age. The duration of this study was 48 days. The Ethical Committee of the Faculty of Veterinary Medicine, Benha University, approved the study protocol (approval number 10518).

Experimental infection

Clostridium perfringens type A was obtained from the Animal Health Research Institute in Dokki, Giza, Egypt. Five groups of broilers were infected with *Clostridium perfringens* at 19 days of age; the birds were challenged via oral gavages with a toxigenic strain of *Clostridium perfringens* type A by inoculation of 1ml of 6×10^8 cfu daily, for three consecutive days (at the 19th, 20th and 21st days of age). The treatments occurred from the 23rd to 27th days of age as described by Bothoko TD (20).

Experimental design

The first group was left uninfected while the other five groups were infected. Group 1: non-infected and non-treated; Group 2: infected and non-treated; Group 3: infected and amoxicillin-treated (20 mg/kg b.wt); Group 4: infected and allicin-treated (25 mg/kg b.wt); Group 5: infected and treated with amoxicillin (20 mg/kg b.wt) and allicin (25 mg/kg b.wt); Group 6: infected and treated with amoxicillin (10 mg/kg b.wt) and allicin (25 mg/kg b.wt). All treatments were administered orally in drinking water for five consecutive days.

Blood samples

Blood samples were collected at the end of 1st, 10th, and 20th day post-drug administration from chicks of each group (which corresponds to 28, 38, and 48 days of age). Six birds from each group were used for the collection of blood samples via wing vein in clean dry tubes. Each blood sample was

divided into two equal parts, and first blood part was collected on heparin and used for haematological studies. The second part was collected in centrifuge tubes; left in a slope position to clot at the room temperature. Clear serum samples were obtained by centrifugation at 2000 g for 10 minutes and transferred carefully in clean dry vials and kept frozen at -20°C until used for biochemical analysis.

Efficacy of the drugs on growth performance

Chicks were individually marked and weighed just prior to infection and weighed on 28th, 38th, and 48th day of age. By subtracting the body weight between two successive weightings for each group, body weight gain was recorded.

Feed consumption and feed conversion were calculated for all groups. The feed conversion was calculated as grams of consumed feed per grams of body weight gain (21). Feed conversion ratio (FCR) was determined as Feed consumption (FC; gm) period/ Weight gain (gm) period.

Effect on haematological parameters

The blood's haematological characteristics, such as red blood cell count (RBCs) (22), white blood cell count (WBCs) (23), haemoglobin (Hb) concentration, and packed cell volume (PCV) (24) were determined.

Effect on biochemical parameters

The serum AST and ALT were measured as previously described (25). Alkaline phosphatase (ALP) (26), serum total proteins (27), serum albumin (28), creatinine and urea were assessed in the serum based on the methods from (29, 30), respectively.

Histopathology

Samples of intestine, liver, and kidney were collected from slaughtered chickens at 28th, 38th, and 48th days of age and fixed in 10% formalin solution for at least 24 hrs. Histopathology was performed according to the methods described in histopathology textbook by Bancroft JD and Gamble M (31). The formalin preserved intestine, liver and kidney tissue were processed in an automated tissue processor. The processing consisted of an

initial 2 step fixation and dehydration. Fixation comprising tissue immersion in 10% buffered formalin for 48 hours, followed by removal of fixative in distilled water for 30 minutes. Dehydration was then carried out by running the tissues through a graded series of alcohol (70%, 90% and 100%). The tissue was initially exposed to 70% alcohol for 120 minutes followed by 90% alcohol for 90 minutes and then two cycles of absolute alcohol, each for one hour. Dehydration was followed by clearing the samples in several changes of xylene. It consisted of tissue immersion for an hour in a mixture comprising 50% alcohol and 50% xylene, followed by pure xylene for one and a half hour. Samples were then impregnated with molten paraffin wax, embedded and blocked out. Paraffin sections (4–5 µm) were stained with hematoxylin and eosin (HE). Stained sections were examined for inflammatory reactions, degenerative and necrotic changes or any other pathological changes in the intestine, liver and kidney of the experimental chickens.

Statistical Analysis

The results were expressed as mean ± SE using the analysis of variance test (one-way ANOVA) followed by Duncan's multiple range test to determine the differences between the averages. All analyses were performed by Statistical Package for Social Science software (SPSS (20) software (SPSS Inc., Chicago, USA).

Results

Clostridium perfringens experimentally infected broiler chickens displayed clinical signs when left untreated. Mild clinical signs appeared 24 to 36 h post-infection. These signs were loss of appetite, drooping wings, diarrhoea, depression, polydipsia, emaciation, dehydration, and ruffled feathers. These clinical signs disappeared under the influence of amoxicillin and/or allicin either alone or in combination.

The effects of amoxicillin and/or allicin on the body weight, body weight gain, FC and FCR of control and infected chickens are shown in Table 1. The effect on total RBCs, WBCs count, Hb content and PCV% in healthy and infected chickens are shown in Table 2. Changes in serum AST, ALT, ALP, total protein, albumin, creatinine and uric acid of control and infected chickens are shown in Tables 3 and Table 4, respectively.

Table 1: The effect of amoxicillin and/or allicin given in drinking water for 5 successive days on growth performance parameters in healthy and experimentally infected broiler chickens with *Clostridium perfringens* at 28th, 38th and 48th days of age (n= 6)

Parameters	Groups	Days post-treatment		
		1 st day	10 th day	20 th day
Body weight (gm)	1	1328±36.11 ^a	1880±9.48 ^a	2332±14.96 ^a
	2	978±60.03 ^c	1350±58.83 ^d	1710±44.27 ^d
	3	1108±55.35 ^b	1568±56.85 ^c	2022±65.86 ^c
	4	1144±24 ^b	1632±28.70 ^{bc}	2104±26.38 ^{bc}
	5	1188±33.82 ^b	1714±42.14 ^b	2206±32.80 ^b
	6	1132±39.29 ^b	1670±47.32 ^{bc}	2146±36.82 ^b
Body weight gain (gm)	1	770.4± 29.29 ^a	552±27.09 ^a	452±24.37 ^a
	2	414.2±65.42 ^c	372±22.89 ^c	360±14.83 ^b
	3	561.8±53.67 ^b	460±20.97 ^{ab}	454±18.42 ^a
	4	594.4±20.86 ^b	488±20.59 ^{ab}	472±27.27 ^a
	5	635.8±35.61 ^b	526±14.00 ^{ab}	492±31.20 ^a
	6	557.2±38.38 ^b	538±28.01 ^a	476±22.49 ^a
Feed consumption (gm)	1	526.2±7.76 ^a	940±21.98 ^a	754±8.98 ^a
	2	423±4.48 ^c	820.4±18.92 ^b	725±23.06 ^{ab}
	3	506.4±2.71 ^b	810.2±21.64 ^b	684.2±14.32 ^b
	4	515.8±5.37 ^{ab}	807.6±11.21 ^b	699.2±11.19 ^b
	5	526±5.18 ^a	822.4±12.13 ^b	704.4±13.09 ^b
	6	518.2±4.91 ^{ab}	811.2±9.61 ^b	695±12.27 ^b
Feed conversion rate (%)	1	0.68±0.26 ^b	1.72±0.18 ^b	1.66±0.09 ^b
	2	1.12±0.06 ^a	2.22±0.28 ^a	2.01±0.15 ^a
	3	0.93±0.05 ^{ab}	1.77±0.18 ^b	1.50±0.07 ^b
	4	0.87±0.25 ^{ab}	1.65±0.11 ^b	1.48±0.04 ^b
	5	0.82±0.14 ^b	1.56±0.12 ^b	1.43±0.04 ^b
	6	0.91±0.12 ^{ab}	1.50±0.12 ^b	1.46±0.05 ^b

Mean values having different letters in the same column for each parameter differ significantly (p<0.05)

Table 2: The effect of amoxicillin and/or allicin given in drinking water for 5 successive days on RBCs, WBCs, Hb and PCV in healthy and experimentally infected broiler chickens with *Clostridium perfringens* at 28th, 38th and 48th days of age (n= 6)

Parameters	Groups	Days post-treatment		
		1 st day	10 th day	20 th day
RBCs ($\times 10^6/\mu\text{l}$)	1	3.87 \pm 0.09 ^a	3.52 \pm 0.21 ^a	3.88 \pm 0.10 ^a
	2	1.94 \pm 0.05 ^c	1.68 \pm 0.05 ^c	1.93 \pm 0.13 ^b
	3	2.89 \pm 0.06 ^b	2.90 \pm 0.03 ^b	2.31 \pm 0.15 ^b
	4	2.85 \pm 0.10 ^b	3.03 \pm 0.09 ^b	2.16 \pm 0.21 ^b
	5	2.72 \pm 0.03 ^b	3.01 \pm 0.03 ^b	2.22 \pm 0.12 ^b
	6	2.82 \pm 0.11 ^b	2.85 \pm 0.05 ^b	2.12 \pm 0.06 ^b
WBCs ($\times 10^3/\mu\text{l}$)	1	22.8 \pm 0.78 ^b	25.1 \pm 0.39 ^c	27.5 \pm 1.91 ^b
	2	39.2 \pm 1.49 ^a	35.2 \pm 1.49 ^a	37 \pm 2.07 ^a
	3	32.6 \pm 2.98 ^b	29.1 \pm 1.31 ^{bc}	28.5 \pm 1.94 ^b
	4	29.6 \pm 0.18 ^b	29 \pm 2.19 ^{bc}	29 \pm 0.52 ^b
	5	28.8 \pm 0.39 ^b	30.6 \pm 2.37 ^{abc}	28.88 \pm 0.39 ^b
	6	28.3 \pm 2.57 ^b	30.2 \pm 2.52 ^{abc}	28.32 \pm 2.57 ^b
Haemoglobin (g/dl)	1	10.62 \pm 1.04 ^a	10.65 \pm 0.36 ^a	10.17 \pm 1.02 ^a
	2	7.74 \pm 0.24 ^b	7.48 \pm 0.20 ^c	7.16 \pm 0.46 ^b
	3	8.37 \pm 0.11 ^b	8.17 \pm 0.56 ^{bc}	9.06 \pm 0.67 ^a
	4	8.65 \pm 0.20 ^b	8.18 \pm 0.32 ^{bc}	10.15 \pm 0.40 ^a
	5	8.48 \pm 0.15 ^b	8.62 \pm 0.31 ^{bc}	9.76 \pm 0.42 ^a
	6	8.82 \pm 0.36 ^b	9.02 \pm 0.33 ^b	9.38 \pm 0.29 ^a
PCV (%)	1	36.05 \pm 2.16 ^a	34.40 \pm 3.15 ^a	33.60 \pm 2.42 ^a
	2	26.40 \pm 1.53 ^b	26.10 \pm 2.36 ^b	26.12 \pm 1.40 ^b
	3	33.10 \pm 2.42 ^a	23.10 \pm 2.42 ^a	29.81 \pm 1.75 ^{ab}
	4	33.75 \pm 1.35 ^a	33.75 \pm 1.35 ^a	30.14 \pm 2.69 ^{ab}
	5	33.06 \pm 1.47 ^a	33.06 \pm 1.47 ^a	30.92 \pm 1.49 ^{ab}
	6	31.41 \pm 0.27 ^a	32.11 \pm 1.85 ^a	30.53 \pm 1.64 ^{ab}

Mean values having different letters in the same column for each parameter differ significantly ($p \leq 0.05$)

Table 3: The effect of amoxicillin and/or allicin given in drinking water for 5 successive days on AST, ALT, ALP and total protein in healthy and experimentally infected broiler chickens with *Clostridium perfringens* at 28th, 38th and 48th days of age (n= 6)

Parameters	Groups	Days post-treatment		
		1 st day	10 th day	20 th day
AST (U/L)	1	184.8±6.76 ^c	174.4±12.1 ^b	196.2±17.7 ^b
	2	317.6±9.81 ^a	284.4±21.4 ^a	383.2±17.1 ^a
	3	238.6±19.9 ^b	207.6±5.70 ^b	211.4±16.1 ^b
	4	226.6±6.53 ^b	209.4±18.4 ^b	214.2±11.5 ^b
	5	224.2±8.48 ^b	196.8±4.93 ^b	225.2±18.4 ^b
	6	232.2±17.8 ^b	211.4±2.01 ^b	223.2±15.7 ^b
ALT (U/L)	1	21.8±1.39 ^c	21.2±0.66 ^b	20.6±0.92 ^b
	2	36.4±2.55 ^a	35.2±2.26 ^a	32.4±1.96 ^a
	3	27.8±1.82 ^b	32.2±1.39 ^b	22.8±1.80 ^b
	4	28.8±2.17 ^b	22.4±1.69 ^b	21.1±0.24 ^b
	5	29.6±2.51 ^{ab}	23.4±2.06 ^b	21.2±1.45 ^b
	6	26.2±2.05 ^b	24.8±2.03 ^b	23.4±2.11 ^b
ALP (U/L)	1	322.6±13.6 ^c	321.2±27.46 ^b	317.8±18.7 ^b
	2	448.2±15.87 ^a	421.2±5.07 ^a	408.6±10.85 ^a
	3	378.6±14.72 ^{ab}	339.4±22.03 ^b	324.2±10.5a ^b
	4	395.2±25.17 ^b	334.4±18.10 ^b	329.8±17.84 ^{ab}
	5	362.6±17.92 ^b	340.8±24.66 ^b	334.6±13.61 ^{ab}
	6	369.2±23.32 ^b	342.6±16.79 ^b	328.2±26.26 ^{ab}
Total protein (mg/dl)	1	5.66±0.12 ^a	5.52±0.11 ^a	5.43±0.09 ^a
	2	4.16±0.05 ^c	4.22±0.05 ^b	4.38±0.10 ^b
	3	4.82±0.09 ^b	4.92±0.21 ^a	5.18±0.30 ^a
	4	4.92±0.37 ^b	5.06±0.22 ^a	5.13±0.37 ^a
	5	4.74±0.10 ^{bc}	4.98±0.30 ^a	5.27±0.21 ^a
	6	5.02±0.31 ^b	5.02±0.29 ^a	5.03±0.19 ^{ab}

Mean values having different letters in the same column for each parameter differ significantly ($p \leq 0.05$)

Table 4: The effect of amoxicillin and/or allcin given in drinking water for 5 successive days on albumin, creatinine and total uric acid in healthy and experimentally infected broiler chickens with *Clostridium perfringens* at 28th, 38th and 48th days of age (n= 6)

Parameters	Groups	Days post-treatment		
		1 st day	10 th day	20 th day
Albumin (g/dl)	1	3.88±0.15 ^a	3.69±0.09 ^a	3.56±0.05 ^a
	2	2.19±0.04 ^c	2.28±0.10 ^c	2.36±0.10 ^c
	3	2.86±0.27 ^b	2.92±0.26 ^b	3.44±0.09 ^{ab}
	4	2.90±0.27 ^b	3.06±0.21 ^b	3.37±0.07 ^{ab}
	5	3.02±0.22 ^b	2.98±0.20 ^b	3.28±0.08 ^b
	6	3.16±0.21 ^b	3.04±0.19 ^b	3.22±0.02 ^b
Creatinine (mg/dl)	1	1.26±0.18 ^c	1.52±0.10 ^c	1.32±0.12 ^b
	2	2.72±0.09 ^a	2.68±0.09 ^a	2.52±0.14 ^a
	3	1.90±0.05 ^b	2.08±0.08 ^b	1.64±0.15 ^b
	4	2.06±0.12 ^b	1.90±0.05 ^b	1.56±0.11 ^b
	5	2.12±0.08 ^b	1.94±0.12 ^b	1.44±0.10 ^b
	6	1.88±0.06 ^b	2.02±0.19 ^b	1.42±0.09 ^b
Uric acid (mg/dl)	1	5.42±0.12 ^b	5.18±0.32 ^b	5.16±0.24 ^b
	2	7.27±0.10 ^a	6.56±0.09 ^a	6.62±0.10 ^a
	3	6.36±0.20 ^c	5.88±0.26 ^{ab}	5.46±0.18 ^b
	4	6.18±0.23 ^c	6.10±0.47 ^{ab}	5.34±0.13 ^b
	5	6.14±0.28 ^c	5.58±0.31 ^{ab}	5.23±0.10 ^b
	6	6.11±0.16 ^c	6.04±0.40 ^{ab}	5.30±0.36 ^b

Mean values having different letters in column for each parameter differ significantly ($p \leq 0.05$)

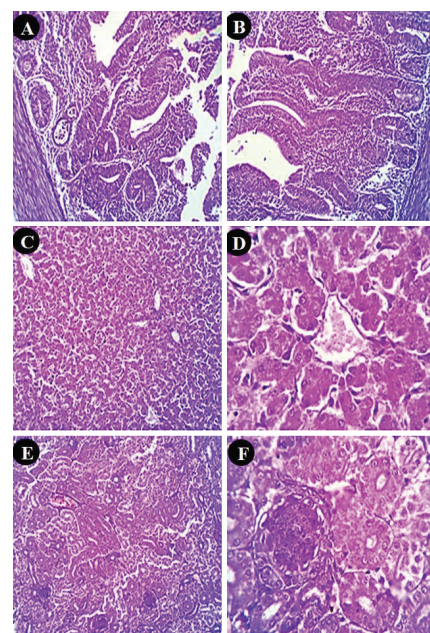


Figure 1: Photomicrograph of chicken's small intestine (A&B), liver (C&D) and kidney (E&F) showing normal histomorphological structure. H&E, (X 200, 400)

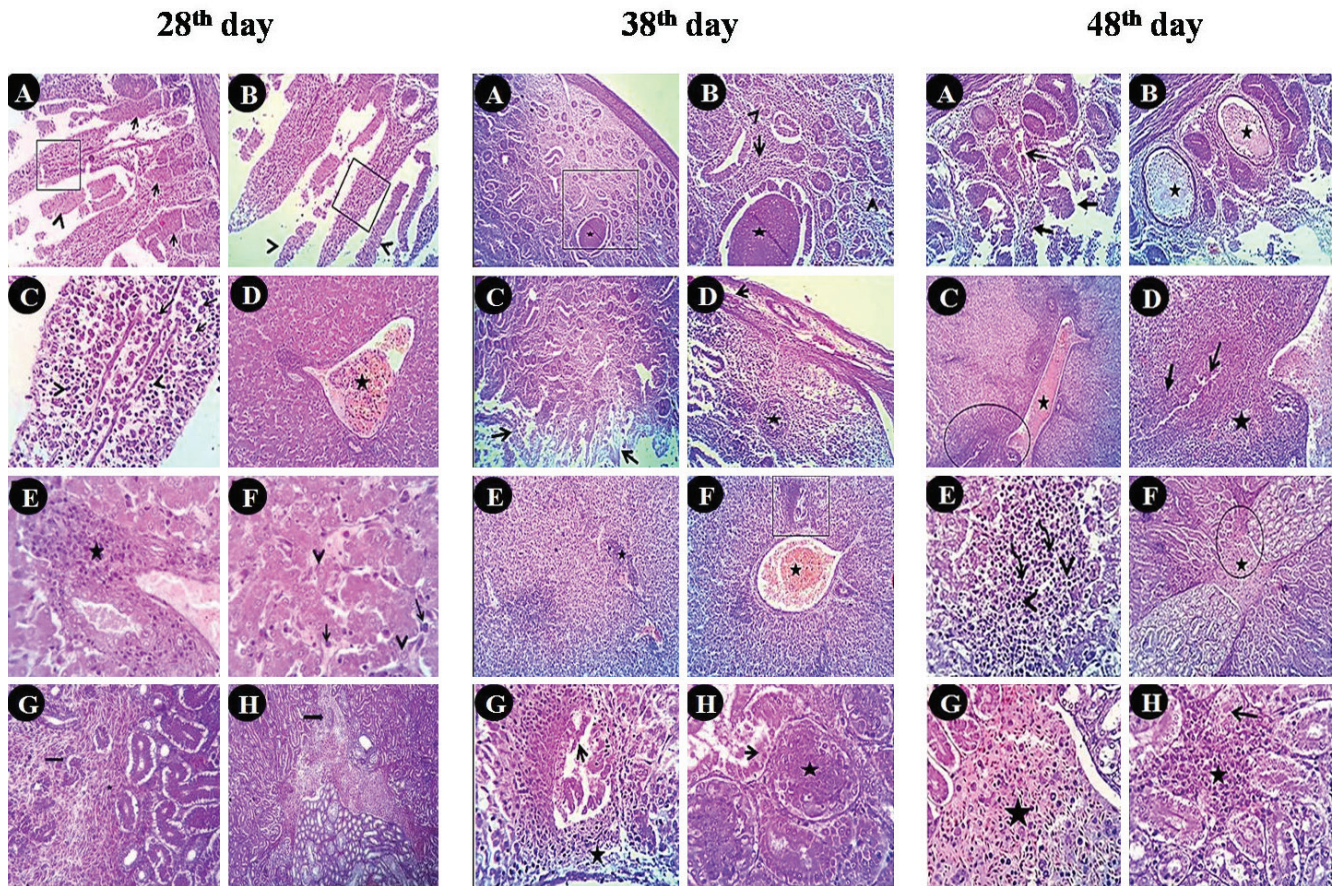


Figure 2: Photomicrograph of chicken's small intestine, liver and kidney of infected non-treated group: H&E

At 28th day (X 100, 200, 400); Intestine: (A&B) showing villous necrosis (square) and sloughing (arrowheads), distorted crypts and glands (arrows), (C) mild infiltration of lymphocytes (arrowheads) and macrophages (arrowheads) in the lamina propria of the villi. Liver: (D) showing congestion of hepatic blood vessels (star), (E) portal aggregation of round cells (lymphocytes, macrophages) (star), (F) mild degenerative changes in most hepatocytes (arrowheads) and hypertrophied Kupffer cells (arrows). Kidney: (G) showing diffuse haemorrhage areas (star) containing scattered necrotic tubules replacing the renal parenchyma (arrow). (H) showing interstitial extravasated erythrocytes containing lymphocytic aggregations (arrow).

At 38th day (X 100, 200, 400); Intestines: (A&B) massive round cell infiltration in the mucosa and submucosa (square & open arrow) with necrotic glands (arrowheads), some glands containing necrotic materials in their centres with cystic dilatation (star). (C) Showing villous necrosis (open arrows), (D) showing lymphoid follicles with necrotic changes (star), congested capillaries and oedema (arrow) in the serosa. Liver: (E) showing portal and interstitial round cell aggregations (star). (F) Moderate congestion of hepatic blood vessels (star). (G)

Mildly hyperplastic bile ducts (arrow), surrounded by large number of round cells (star). Kidney: (H) showing necrotic changes in the tubular epithelium (arrow) with hypertrophic and hyperplastic mesangial and endothelial cells in some glomeruli (star).

At 48th day (X 100, 200); Intestine: (A&B) showing villous necrosis (closed arrows), congested mucosal and submucosal blood vessels (open arrow). Some of the intestinal glands were cystic and filled by secretory material and degenerated cells (stars). Liver: (C) showing massive portal and perivascular round cell infiltration (circle) and congested hepatic blood vessels (star). (D) Hyperplastic bile ducts (open arrow) surrounded by fibrosis (closed arrow) and large number of round cells (star) mainly lymphocytes (arrowheads) and macrophages (curved arrow). Kidney: (F&G) Showing a large mass of hepatoid like structure (star). (H) Showing focal degenerative and necrotic changes in some tubular epithelium (open arrow) and focal interstitial aggregation of round cells (star).

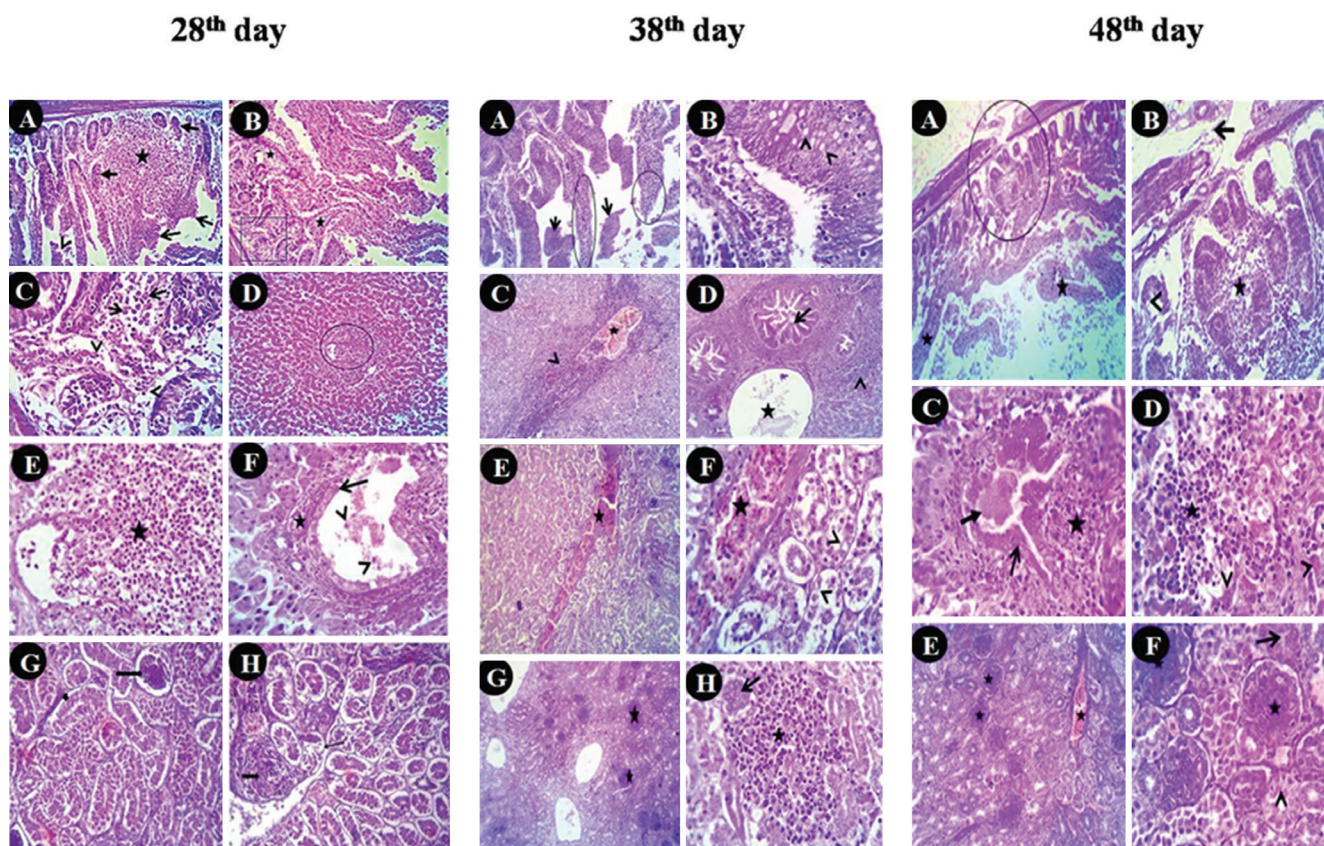


Figure 3: Photomicrograph of chicken's small intestine, liver and kidney of infected and amoxicillin treated group: H&E

At 28th day (X 200, 400); Intestine: (A&B) showing villous necrosis (open arrows), desquamation of the epithelial lining (arrowhead), Focal distortion and degeneration of the intestinal crypts and gland (closed arrows) and (C) moderate infiltration of round cells in the lamina propria and sub-mucosa (stars). (C) Lymphocytes (arrowheads) and macrophages (open arrows). Liver: (D&E) showing focal hepatic necrosis especially periportal (circle) which replaced by moderate aggregation of round cells (star). (F) Showing hyperplasia of bile ducts (open arrow) with partial destruction of the epithelial lining (arrowhead) and periductal fibrosis (star). Kidney: (G) showing dissociated tubular epithelium (arrowhead) and contracted glomeruli (arrow). (H) Showing regenerative attempts (thick arrow) and thickened tubular basement membrane (thin arrow).

At 38th day (X 100, 200, 400); Intestine: (A&B) showing villous necrosis (circle), sloughed epithelium (arrows) and focal goblet cell metaplasia (arrowheads). Liver: (C&D) showing biliary hyperplastic changes (open arrow), massive round cells infiltration in the portal area (arrowheads) and congestion of hepatic blood vessels (stars). Kidney: (E&F) showing dilatation of the renal blood vessels (star), Focal necrotic changes

in some tubular epithelium (arrowheads), (G) Most of the glomeruli showing mild to moderate proliferative reactions in the mesangial and endothelial cells (stars). (H) Focal regenerative tubules (arrow) beside focal aggregation of round cells (star).

At 48th day (X 100, 200, 400); Intestine: (A) showing widespread villous necroses (star), (B) moderate round cells infiltration in the mucosa and sub-mucosa (star), glandular and crypt distortion (arrowhead), edematous in the muscular and sub-serosa (open arrow). Liver: (C) showing mild to moderate round cell aggregation in the portal area (star) with mild biliary hyperplasia (open arrow) and presence of static secretory materials in their lumina (closed arrow). (D) Multifocal interstitial round cells infiltration (star) with necrotic changes in some hepatocytes (arrowheads). Kidney: (E) showing mild to moderate congestion of renal blood vessels and capillaries (stars). (F) Focal degenerative (open arrow) and necrotic changes (arrowhead) in some tubular epithelium. Some glomeruli show mesangial and endothelial hyperplastic and hypertrophied changes (stars)

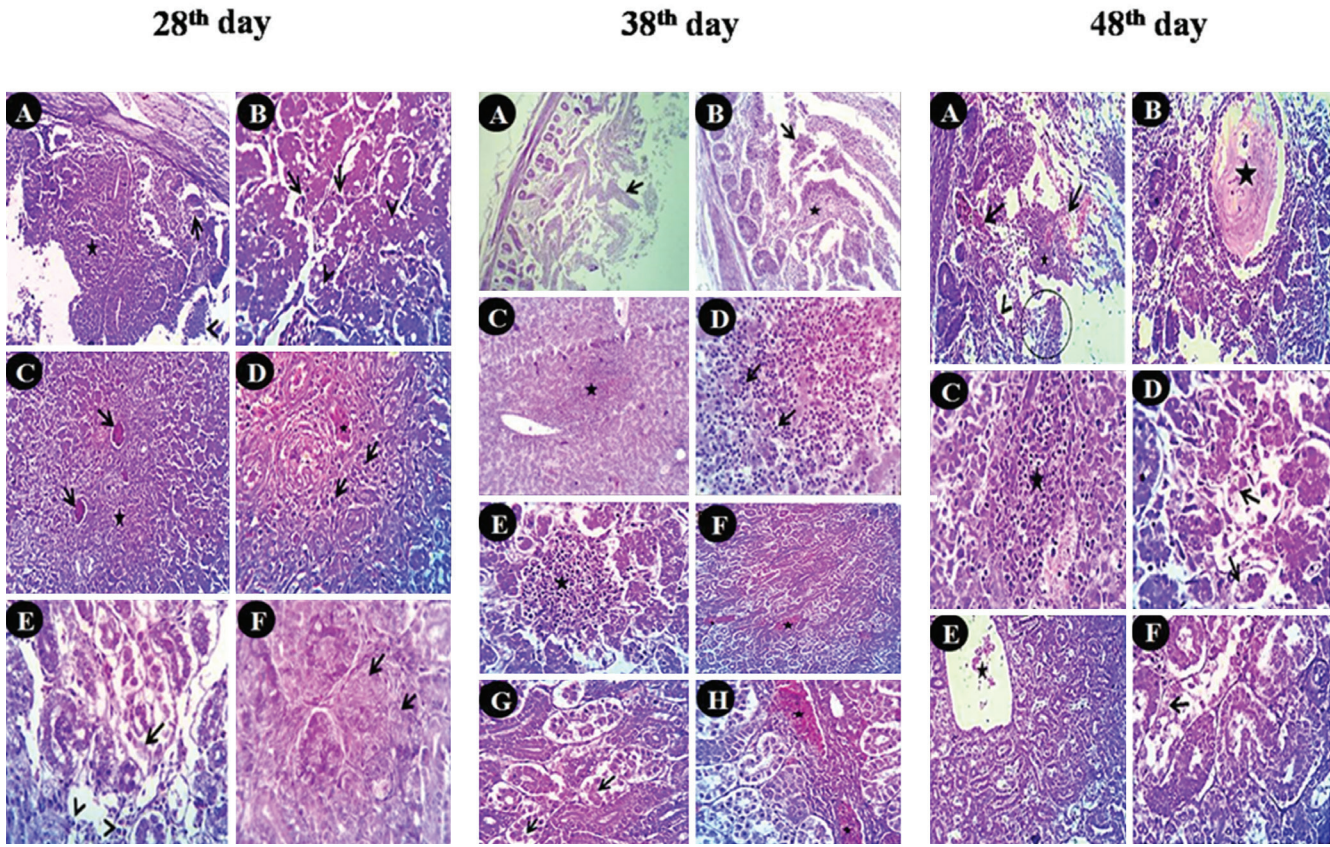


Figure 4: Photomicrograph of chicken's small intestine, liver, and kidney of infected and allicin treated group: H&E

At 28th day (X 200, 400); Intestine: (A) showing villous necrosis (star), desquamation (arrowhead) and crypt distortion (open arrow). Liver: (B) showing hypertrophied Kupffer cells (open arrows), fatty change in a number of the hepatocytes (arrowheads). (C) Congested hepatic blood vessels (arrows) with portal fibroblasts proliferation (star) and (D) round cells infiltration, mainly lymphocytes (open arrow). Kidney: (E) showing focal degenerative and necrotic changes in some tubular epithelium (open arrow), mild interstitial round cell infiltration (arrowheads). (F) Focal regeneration in some tubular epithelium (open arrow)

At 38th day (X 100, 200, 400); Intestine: (A&B) showing villous necrosis (open arrows) with moderate round cell infiltration in the mucosa and submucosa (star). Liver: (C&D) showing portal and interstitial round cells aggregation (star) mainly lymphocytes (open arrows). Kidney: (F&G&H) showing focal necrotic changes in some renal tubular epithelium (arrows) with congested renal blood vessels (stars)

At 48th day (X 100, 200); Intestine: (A&B) Intestine: (A) showing massive villous necroses (circle), dilated capillaries (open arrows) in the mucosa and submucosa with moderated round cells infiltration (star). (B) Some of the intestinal crypts are cystically dilated and filled with mucinous secretion (star) Liver: (C&D) showing interstitial aggregation of round cells (star), necrotic changes in some hepatocytes (open arrow). Kidney: (E&F) showing moderately congested renal blood vessels (star) with focal necrotic changes in some tubular epithelium (open arrow)

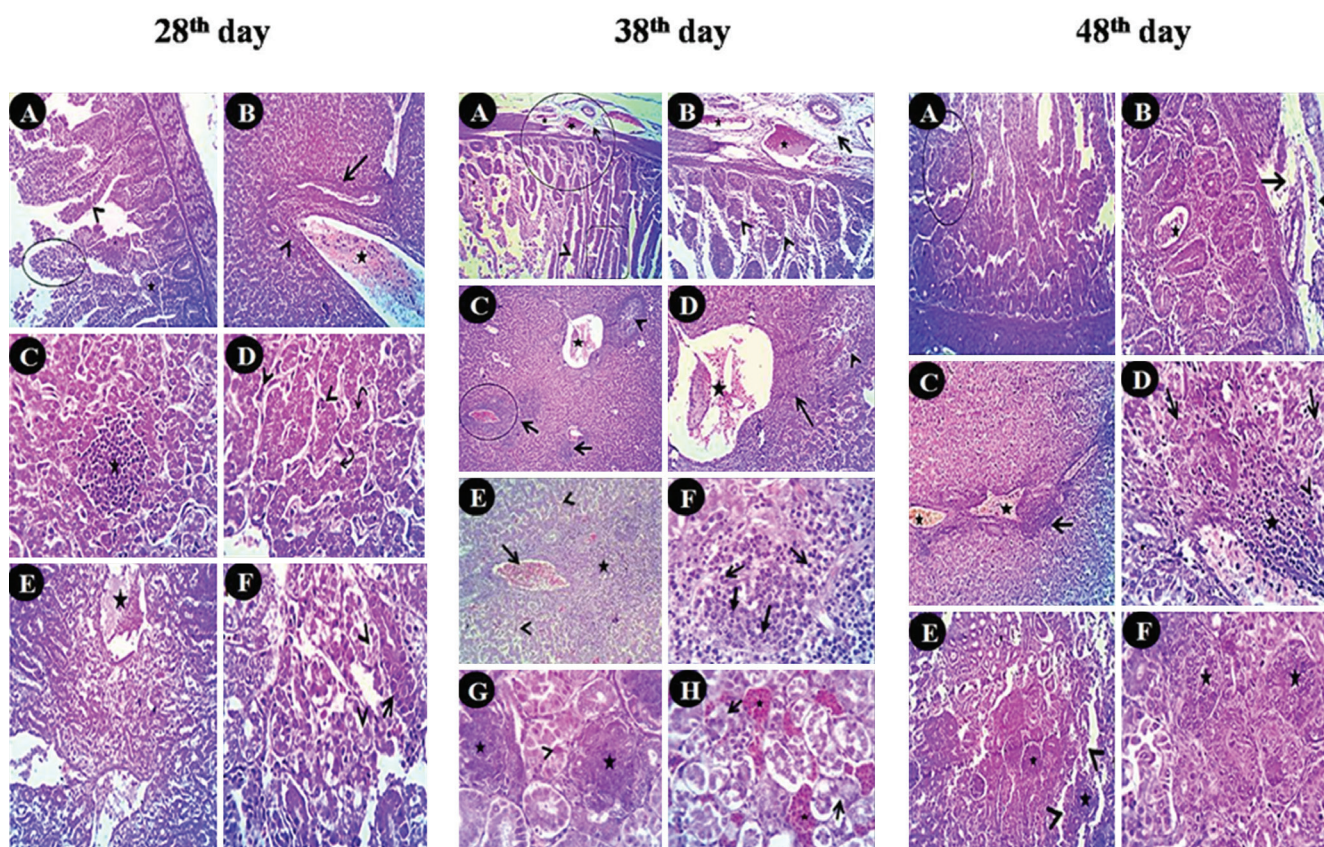


Figure 5: Photomicrograph of chicken's small intestine, liver and kidney of infected and treated with 20 mg amoxicillin and 25 mg allacin/kg b.wt. H&E

At 28th day (X 100, 200, 400); Intestine: (A) showing villous necrosis (circle), desquamation (arrowhead) and round cell infiltration in the mucosa (star). Liver: (B) showing congested hepatic blood vessels (star), portal biliary (open arrow) and fibroblast proliferation (arrowhead). (C&D) showing focal interstitial aggregation of round cells (star) and dilated sinusoids with hypertrophied kupffer cells (arrowheads), degenerative changes in some hepatocytes (curved arrows). Kidney: (E&F) showing moderately congested renal blood vessels (star). Focal degenerative and necrotic changes in tubular epithelium (arrowheads) and focal regenerative processes in some tubules (open arrow).

At 38th day (X 100, 200, 400); Intestine: (A&B) showing villous necrosis (square), crypt and gland destruction (arrowheads), the muscular coat and the subserosal tissue showing congested blood vessels (stars) and exudative oedema (open arrows). Liver: (C&D) showing moderate to severe vascular congestion (star) with prominent lymphocytosis in portal areas (open arrows) and bile duct hyperplasia (arrowheads). (E&F) portal and interstitial round cells infiltration (star) with partial replacement of the hepatocytes by lymphocytes (open

arrow) and macrophages (closed arrow), necrotic changes in most parenchyma (arrowheads). Kidney: (H) showing moderate congestion of intertubular capillaries (star) with focal degenerative and necrotic changes in some tubular epithelium (open arrows), (G) some glomeruli showed hypertrophic and hyperplastic mesangial and endothelial cells (stars).

At 48th day (X 100, 200, 400); Intestine: (A&B) showing characteristic villous necrosis (circle). The crypts and the glands are cystically dilated and filled by necrotic debris (star), muscular coat showing focal vascular dilatation (arrowhead) and exudative edematous reaction (open arrow). Liver: (C) showing mild to moderate congestion of hepatic blood vessels (stars) with round cells infiltration in the portal area (open arrow). (D) Higher magnification of the previous figure to show hydropic degeneration (open arrows) and infiltration of the portal area by mononuclear cells (star) mainly lymphocytes (arrowhead). Kidney: (E) showing necrotic changes in some tubules (arrowheads) and glomerular hyperplastic mesangial and endothelial cells (stars). (F) Regenerative changes of some tubular epithelium (stars).

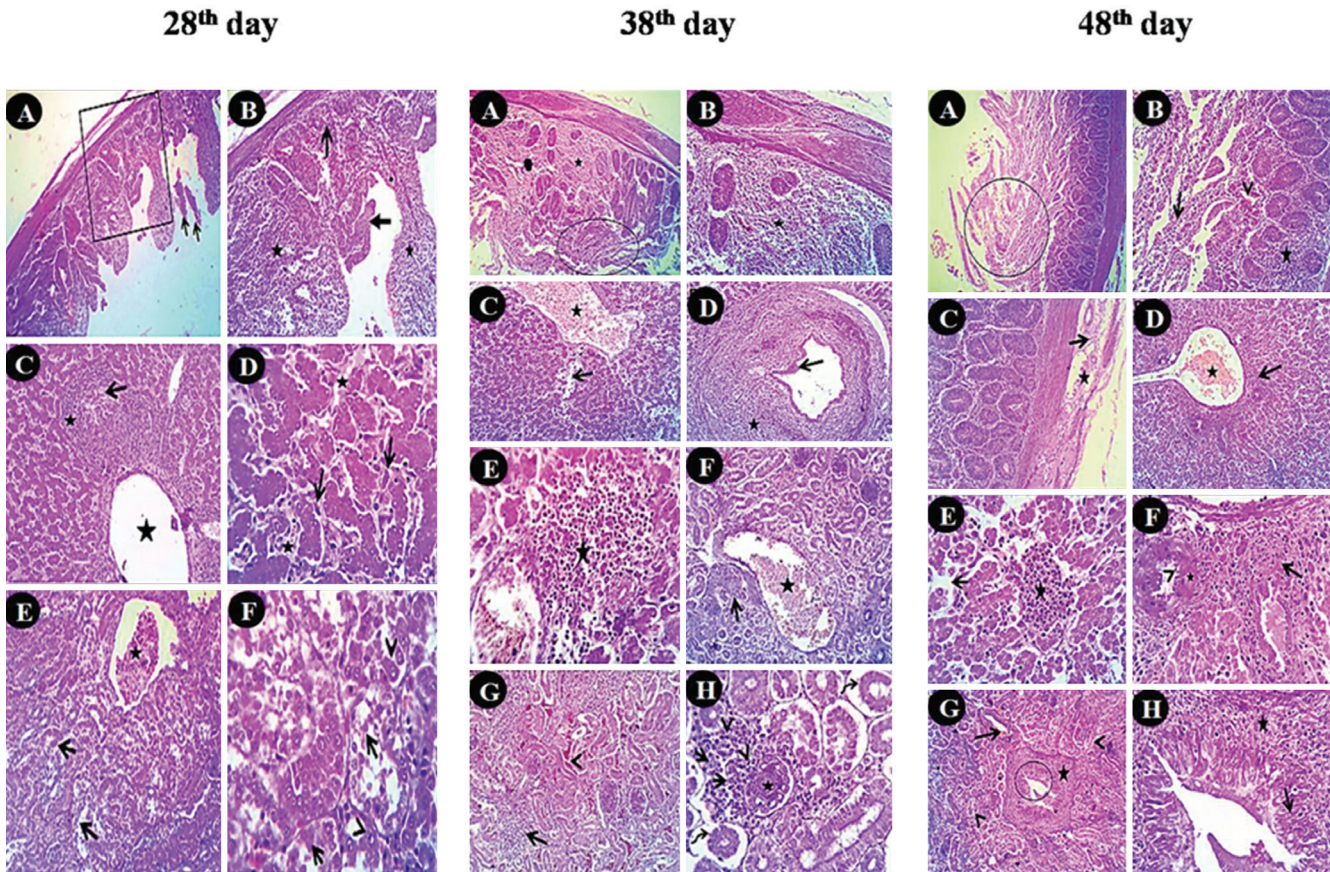


Figure 6: Photomicrograph of chicken's small intestine, liver and kidney of infected and treated with 10 mg amoxicillin and 25 mg allicin/kg b.wt. H&E

At 28th day (X 100, 200, 400); Intestine: (A) showing villous atrophy and desquamated epithelium (open arrows), (B) villous necrosis (closed arrow), gland distortion (open arrow), round cells infiltration in the mucosa and submucosa (star) and intermuscular edema (arrow head). Liver: (C) showing portal biliary hyperplasia (open arrow) with massive round cell infiltration (star), congested hepatic blood vessels (star), (D) dilated sinusoids (stars) and hypertrophied Kupffer cells (open arrow). Kidney: (E&F) showing moderate congestion of renal blood vessels (star) and focal degenerative (arrow heads) and necrotic changes (open arrows) in some tubular epithelium.

At 38th day (X 100, 200); Intestine: (A&B) showing villous necrosis and epithelial sloughing (circle). Moderate infiltration of the mucosa, submucosa and muscular coat by round cells (stars). Liver: (C) showing moderately congested hepatic blood vessels (star) and sinusoids (arrow). (D&E) Severe biliary hyperplasia (open arrow) with periductal fibrosis and round cell infiltration (star). Kidney: (F&G) showing moderate to severe congestion of renal blood vessels (star), intertubular capillaries (arrowhead) with multifocal interstitial round cell aggregations (open arrow). (H) Focal degenerative

and necrotic changes in renal tubular epithelium with detached basement membrane (curved arrows) and interstitial aggregation of macrophages (arrow) and lymphocytes (arrowheads) and hyaline casts within renal tubules (star).

At 48th day (X 100, 200, 400); Intestine: (A&B) showing widespread villous necroses (circle) with moderate round cells infiltration in the mucosa and submucosa (star) and dilated blood vessels (arrowhead), (C) exudative edematous changes in the tunica muscularis (open arrow) with congested blood vessels (star). Liver: (D) showing mild to moderate vascular congestion (star) with mild to moderate round cells infiltration in the portal area (open arrow) and (E) in the interstitial tissue (star) beside dilated sinusoids (open arrow). (F) Some of the hepatic arterioles showing vacuolated endothelium (arrowhead) and thick hyalinized walls (star) beside hyalinized fibrosis in the portal area (open arrow). Kidney: (G) showing necrotic changes in the tubular epithelium (arrowhead), hyperplastic changes in the ducts (open arrows) which surrounded by a moderate number of round cells (stars).

Histopathological changes were observed in the intestine, liver, and kidneys of all groups at 28, 38, and 48 days of age; however, in comparison to the control group (Figure 1), all groups infected with *Clostridium perfringens* showed different grades of lesions. Lesions were the most severe in the group, infected but not treated with either amoxicillin and/or allicin (Figure 2), while they were milder in groups treated with amoxicillin and/or allicin (Figure 3, Figure 4, Figure 5, Figure 6).

Lesions in the intestines consisted of villous necrosis, epithelial desquamation, distorted crypts and glands, congestion, oedema and mild infiltration of the propria with lymphocytes and macrophages. Liver showed congestion of hepatic blood vessels, portal aggregation of lymphocytes and macrophages, mild degenerative changes (cloudy swelling, hydropic degeneration) in most hepatocytes, and hypertrophied Kupffer cells. Kidney lesions included diffuse haemorrhagic areas containing scattered necrotic tubules, and interstitium infiltrated with erythrocytes and lymphocytic aggregations.

Discussion

Broiler chickens experimentally infected with *Clostridium perfringens* had significant decrease in body weight and weight gain, and increase in feed conversion rate. Similar results were reported in several studies (32, 33), in which the authors described hepatitis, associated with high incidence of *Clostridium perfringens* infections in broiler flocks. Beside hepatitis, they have also observed in the same study a decrease in the growth rate, an increased feed conversion rate and necrotic enteritis. Clostridial toxins induce damage in intestinal tissue and the liver, which leads to a decrease in a nutrient absorption and metabolism, and consequently reduces growth performance (33).

The effects of the treatments in our study, which are presented in Table 1, Table 2 and Table 3 and Figures 2 to 6, revealed that the administration of amoxicillin and/or allicin for the treatment of *Clostridium perfringens* infection resulted in improved growth performance parameters, and milder lesions in the intestines, liver and kidney. This improvement is likely due to the antimicrobial effect of the antibiotic used, resulting in decreased intestinal colonization in diseased broilers, prevention of necrotic enteritis and consequently

increased body weight, weight gain, and improved feed conversion rate (34). Furthermore, the infected chickens showed an improvement in body weight gain and FCR when treated with amoxicillin (35). The activities of intestinal mucosa enzymes and nutrient digestibility were increased after garlic supplementation and represent an alternative to antibiotics in broiler nutrition (36). It was reported before that diets supplemented with garlic at a dose of 1 and 1.5 gm/kg diet prevent subclinical necrotic enteritis and improved performance of broiler chickens (37).

A considerable decrease was noted in the total number of erythrocytes, haemoglobin concentration and packed cell volume percentage in infected broiler chickens when compared to non-infected, untreated broiler chickens. These results might be due to excessive destruction of erythrocytes by the clostridial toxin (38). The results of our study also indicate that *Clostridium perfringens* infection in broiler chickens induced a significant increase in the total number of leukocytes. Changes in leukocytes in broiler chickens infected with *Clostridium perfringens* are likely a reflection of the inflammatory response in the intestinal tract due to infection. Interestingly, significant increases in the PCV, Hb, and RBCs of chicken feed with garlic had been previously reported (39).

Infected and untreated chickens displayed significant elevation in liver enzyme activity (AST, ALT, and ALP) in comparison to non-infected untreated chickens. This elevation might be due to pathological changes in liver post infections or due to clostridial toxin-induced alteration in cellular permeability, which allows the escape of liver enzymes into the serum (38). Infected broiler chickens treated with amoxicillin and/or allicin displayed significant elevation in the activity of AST, ALT, and ALP at the 28th day when compared to healthy non-treated broiler chickens. These results are similar to those reported by Bryan C et al. (40) who reported that improved liver enzymes post-treatment infection in chickens might be due to an antimicrobial effect of the drugs used in suppression microorganisms invading the host and retarding its metabolic activity and liver enzyme activity. These findings might be attributed to the antioxidant effect of garlic (41). In infected and untreated chickens, there was a significant reduction in total protein and albumin levels in blood. Hypoalbuminemia could be due

to the destructive effect of the microorganism and clostridial toxins on the liver cells producing albumin. The reduction in total protein and albumin in the infected broiler chickens might be due to the malabsorption of nutrients from the inflamed intestines. Another explanation for the reduction in total protein and albumin in broilers infected with *Clostridium perfringens* comes from a study of Lovland A et al., in which the authors reported similar changes of protein picture in broilers infected with *Clostridium perfringens* (33).

Infected chickens treated with amoxicillin displayed an insignificant decrease in total protein blood content in comparison to the healthy non-treated chickens but had significant decreases in albumin concentration. This improvement in serum protein might be due to the improved state of the liver in the treated chickens as a synthesis of albumin; the largest individual protein fraction in avian plasma takes place in the liver, or alternatively, treatment alters the renal secretion by changing the state of the kidney (38). The infected and allacin treated group showed non-significant changes in total proteins and albumin at 2nd-week post-treatment in comparison to the control group. These results indicate an improvement in the hepatic functions due to the antioxidant effect of the phytophenolic compounds in garlic (42).

A marked increase in creatinine and uric acid levels was recorded after experimental infection. Increase in uric acid, creatinine in the infected birds might be a result of degenerative changes in the kidney tubules, preventing the excretion of uric acid and creatinine, increasing their levels in serum. Our data are also in accordance with the finding of Harrison et al. (43), who reported an increase in creatinine level in case of renal disease. Garlic reduced urea, uric acid, and creatinine levels after lead toxicity in broiler chickens (44).

The pathological lesions in chickens infected with *Clostridium perfringens* were similar as were observed and described before (47, 48). Findings in the liver and kidneys in our study were similar to those reported before for these organs in chickens 12 h after inoculation of broth culture or toxins of *Clostridium perfringens* (49).

Conclusions

The combination of both drugs (amoxicillin and allacin) proved to be the better treatment of *Clostridium perfringens* infection than each drug alone, indicating a synergistic effect. No significant differences between the two doses of amoxicillin with allacin were detected. This combination improved the health state, body weight gain, feed conversion rate, blood parameters and biochemical indices, and reduced the severity of histopathological changes in the intestines, liver and kidney.

Acknowledgement

The authors wish to thank Prof. Elsayed Rashad Abdelmegeed, Professor of Pathology, Faculty of Veterinary Medicine, Zagazig University, Egypt, for his help in histopathological examination. This work was funded by Researchers Supporting Project number (RSP-2019/121), King Saud University, Riyadh, Saudi Arabia.

References

1. Collier C, Van der Klis J, Deplancke B, Anderson D, Gaskins H. Effects of tylosin on bacterial mucolysis, *Clostridium perfringens* colonization, and intestinal barrier function in a chick model of necrotic enteritis. *Antimicrob Agents Chemother* 2003; 47: 3311–7.
2. Kaldhusdal M, Schneitz C, Hofshagen M, Skjerve E. Reduced incidence of *Clostridium perfringens*-associated lesions and improved performance in broiler chickens treated with normal intestinal bacteria from adult fowl. *Avian Dis* 2001; 45: 149–56.
3. Saif YM, ed. *Diseases of poultry*. 11th ed. Ames : Iowa State Press ; Blackwell Publishing Company, 2003.
4. Gazdzinski P, Julian R. Necrotic enteritis in turkeys. *Avian Dis* 1992; 36: 792–8.
5. Brennan J, Moore G, Poe S, et al. Efficacy of in-feed tylosin phosphate for the treatment of necrotic enteritis in broiler chickens. *Poult Sci* 2001; 80: 1451–4.
6. Amin A, El-Ansary A, Issa Y. Colorimetric determination of amoxycillin in pure form and in pharmaceutical preparations. *Talanta* 1994; 41: 691–4.

7. Nagaralli B, Seetharamappa J, Melwanki M. Sensitive spectrophotometric methods for the determination of amoxicillin, ciprofloxacin and piroxicam in pure and pharmaceutical formulations. *J Pharm Biomed Anal* 2002; 29: 859–64.
8. Ross Z, O’Gara EA, Hill DJ, Sleightholme H, Maslin DJ. Antimicrobial properties of garlic oil against human enteric bacteria: evaluation of methodologies and comparisons with garlic oil sulfides and garlic powder. *Appl Environ Microbiol* 2001; 67: 475–80.
9. Alli J, Boboye B, Okonko I, Kolade A, Nwanze J. *In-Vitro* assessments of the effects of garlic (*Allium sativum*) extract on clinical isolates of *Pseudomonas aeruginosa* and *Staphylococcus aureus*. *Adv Appl Sci Res* 2011; 2: 25–36.
10. Durairaj S, Srinivasan S, Lakshmanaperumalsamy P. *In vitro* antibacterial activity and stability of garlic extract at different pH and temperature. *E J Bio* 2009; 5: 5–10.
11. Stanačev V, Glamović D, Miloscaron N, Puvača N, Stanačev V, Plavscaron N. Effect of garlic (*Allium sativum* L.) in fattening chicks nutrition. *Afr J Agric Res* 2011; 6: 943–8.
12. Iji PA, Saki A, Tivey DR. Body and intestinal growth of broiler chicks on a commercial starter diet. 1. Intestinal weight and mucosal development. *Br Poult Sci* 2001; 42: 505–13.
13. Macpherson LJ, Geierstanger BH, Viswanath V, et al. The pungency of garlic: activation of TRPA1 and TRPV1 in response to allicin. *Curr Biol* 2005; 15: 929–34.
14. Block E, Dane AJ, Thomas S, Cody RB. Applications of direct analysis in realtime mass spectrometry (DART-MS) in *Allium* chemistry. 2-propenesulfenic and 2 propenesulfinic acids, diallyl trisulfane S-oxide, and other reactive sulphur compounds from crushed garlic and other *Alliums*. *J Agric Food Chem* 2010; 58: 4617–25.
15. Qureshi AA, Abuirmeileh N, Din ZZ, Elson CE, Burger WC. Inhibition of cholesterol and fatty acid biosynthesis in liver enzymes and chicken hepatocytes by polar fractions of garlic. *Lipids* 1983; 18: 343–8.
16. Ankri S, Mirelman D. Antimicrobial properties of allicin from garlic. *Microbes Infect* 1999; 1(2): 125–9.
17. Cho SJ, Rhee DK, Pyo S. Allicin, a major component of garlic, inhibits apoptosis of macrophage in a depleted nutritional state. *Nutrition* 2006; 22: 1177–84.
18. Marien M, Nauwynck H, Duchateau L, et al. Comparison of the efficacy of four antimicrobial treatment schemes against experimental *Ornithobacterium rhinotracheale* infection in turkey poult pre-infected with avian pneumovirus. *Avian Pathol* 2006; 35: 230–2.
19. Robyn J, Rasschaert G, Hermans D, Pasmans F, Heyndrickx M. Is allicin able to reduce *Campylobacter jejuni* colonization in broilers when added to drinking water?. *Poult Sci* 2013; 92: 1408–18.
20. Botlhoko TD. Performance of *Clostridium perfringens*-challenged broilers inoculated with effective microorganisms. Pretoria : Faculty of Natural and Agricultural Sciences. University of Pretoria, 2009. Masters dissertation
21. Wanger D, Furrow R, Bradley B. Subchronic toxicity of growth promoters in broiler chickens. *Vet Pathol* 1983; 20: 353–9.
22. Hepler OE. Manual of clinical laboratory methods. Calif Med 1949; 70: 310–1.
23. Lucas AM, Jamroz C. Atlas of avian hematology. Agriculture monography, 25. Washington : United States Department of Agriculture, 1961.
24. Eilers RJ. Notification of final adoption of an international method and standard solution for hemoglobinometry specifications for preparation of standard solution. *Am J Clin Pathol* 1967; 47: 212–4.
25. Retiman S, Frankel S. Calorimetric method for the determination of blood, aminotransferase enzymatic activities. *Am J Clin Pathol* 1957; 28: 56–63.
26. Kind P, King E. Estimation of plasma phosphatase by determination of hydrolysed phenol with amino-antipyrine. *J Clin Pathol* 1954; 7: 322.
27. Weichselbaum T. An accurate and rapid method for the determination of proteins in small amounts of blood serum and plasma. *Am J Clin Pathol* 1946; 10: 40–9.
28. Doumas BT, Watson WA, Biggs HG. Albumin standards and the measurement of serum albumin with bromocresol green. *Clin Chim Acta* 1971; 31: 87–96.
29. Bartels H, Böhmer M, Heierli C. Serum creatinine determination without protein precipitation. *Clin Chim Acta* 1972; 37: 193–7.
30. Sampson EJ, Baird MA, Burtis C, Smith EM, Witte D, Bayse DD. A coupled-enzyme equilibrium method for measuring urea in serum: optimization and evaluation of the AACC study group on urea candidate reference method. *Clin Chem* 1980; 26: 816–26.

31. Bancroft JD, Layton C. The hematoxylin and eosin. In: Suvarna SK, Layton C, Bancroft JD, eds. Bancroft's theory and practice of histological techniques. 7th ed. Philadelphia : Churchill Livingstone /Elsevier, 2013: 173–86.
32. Lovland A, Kaldhusdal M. Severely impaired production performance in broiler flocks with high incidence of *Clostridium perfringens*-associated hepatitis. Avian Pathol 2001; 30: 73–81.
33. Lovland A, Kaldhusdal M. Liver lesions seen at slaughter as an indicator of necrotic enteritis in broiler flocks. FEMS Immunol Med Microbiol 1999; 24: 345–51.
34. Watkins K, Shryock T, Dearth R, Saif Y. *In-vitro* antimicrobial susceptibility of *Clostridium perfringens* from commercial turkey and broiler chicken origin. Vet Microbiol 1997; 54: 195–200.
35. Lanckriet A, Timbermont L, De Gussem M, et al. The effect of commonly used anticoccidials and antibiotics in a subclinical necrotic enteritis model. Avian Pathol 2010; 39: 63–8.
36. Peinado M, Ruiz R, Echávarri A, Aranda-Olmedo I, Rubio L. Garlic derivative PTS-O modulates intestinal microbiota composition and improves digestibility in growing broiler chickens. Anim Feed Sci Technol 2013; 181: 87–92.
37. Jimoh A, Ibitoye E, Dabai Y, Garba S. *In vivo* antimicrobial potentials of garlic against *Clostridium perfringens* and its promotant effects on performance of broiler chickens. Pak J Biol Sci 2013; 16: 1978–84.
38. Coles E. Veterinary clinical pathology. 4th ed. Philadelphia : WB Saunders, 1986.
39. Oleforuh-Okoleh VU, Ndofor-Foleng HM, Olorunleke SO, Uguru JO. Evaluation of growth performance, haematological and serum biochemical response of broiler chickens to aqueous extract of ginger and garlic. J Agric Sci 2015; 7: 167–73.
40. Bryan C, John J, Ingrid A, Brend S, Robrecht F. Comparison of the efficacies of three fluoroquinolone, one of antimicrobial agents, given as continuous or pulsed-water medication, against *Escherichia coli* infection in chickens. Antimicrob Agents Chemother 1998; 42: 83–7.
41. Jackson R, McNeil B, Taylor C, Holl G, Ruff D, Gwebu E. Effect of aged garlic extract on caspase-3 activity, *in vitro*. Nutr Neurosci 2002; 5: 287–90.
42. Chen S, Shen X, Cheng S, et al. Evaluation of garlic cultivars for polyphenolic content and antioxidant properties. PLoS One 2013; 8: e79730. doi: 10.1371/journal.pone.0079730.
43. Harrison G, Harrison L. Clinical avian medicine and surgery. Philadelphia ; London : WB Saunders Company, 1986.
44. Hossain MA, Akanda MR, Mostofa M, Awal MA. Therapeutic competence of dried garlic powder (*Allium sativum*) on biochemical parameters in lead (Pb) exposed broiler chickens. J Adv Vet Anim Res 2014; 1: 189–95.
45. Gholamiandehkordi AR, Timbermont L, Lanckriet A, et al. Quantification of gut lesions in a subclinical necrotic enteritis model. Avian Pathol 2007; 36: 375–82.
46. Pedersen K, Bjerrum L, Heuer OE, Lo Fo Wong DM, Nauerby B. Reproducible infection model for *Clostridium perfringens* in broiler chickens. Avian Dis 2008; 52: 34–9.
47. Das B, Dutta G, Devriese L, Phykan A. Necrotic enteritis in chickens due to field isolates of *Clostridium perfringens* type A. Indian J Vet Pathol 1997; 21: 27–9.
48. Olkowski AA, Wojnarowicz C, Chirino-Trejo M, Drew MD. Responses of broiler chickens orally challenged with *Clostridium perfringens* isolated from field cases of necrotic enteritis. Res Vet Sci 2006; 81: 99–108.
49. Immerseel FV, Buck JD, Pasmans F, Huyghebaert G, Haesebrouck F, Ducatelle R. *Clostridium perfringens* in poultry: an emerging threat for animal and public health. Avian Pathol 2004; 33: 537–49.

EFFICACY OF AMOXICILLIN (ATCOMOX®) AND/OR ALLICIN ON PERFORMANCE, HAEMATOLOGICAL, BIOCHEMICAL, AND HISTOPATHOLOGICAL CHANGES IN *CLOSTRIDIUM PERFRINGENS* INFECTED CHICKENS

M. Aboubakr, A. Elkomy, S. Belih, M. Morad, H. Shaheen, M. M. Abdel-Daim

Povzetek: V študiji smo ugotavljali učinkovitost amoksicilina in/ali alicinina pri zdravih pitovnih piščancih in pitovnih piščancih poskusno okuženimih z bakterijo *Clostridium perfringens*. Piščanci so bili razdeljeni v šest skupin in so zdravila dobivali peroralno preko vode pet dni zapored. V prvi skupini so bili neokuženi in nezdravljeni piščanci, v drugi okuženi in nezdravljeni, v tretji okuženi in zdravljeni z amoksicilinom (20 mg/kg telesne mase), v četrti skupini okuženi in zdravljeni z alicinom (25 mg/kg telesne mase) v peti skupini okuženi in zdravljeni z amoksicilinom (20 mg/kg teže) in alicinom (25 mg/kg telesne mase) in v šesti skupini okuženi in zdravljeni z amoksicilinom (10 mg/kg teže) in alicinom (25 mg/kg telesne mase). Spremljali smo prirast piščancev ter njihove hematološke in biokemične parametre. Pri okuženih piščancih smo v krvi opazili znatno znižanje skupnih beljakovin, albuminov, RBC, Hb in PCV ter znatno povečanje WBC, AST, ALT, ALP, kreatinina in sečne kisline. Uporaba amoksicilina in/ali alicina za zdravljenje okužbe s *Clostridium perfringens* je povzročila izboljšanje hematoloških in biokemičnih sprememb po okužbi. Odmerek amoksicilina 10 mg/kg in alicina 25 mg/kg telesne mase za zdravljenje okužbe s *Clostridium perfringens* pri pitovnih piščancih brojlerjih se je izkazal kot najbolj učinkovit, verjetno zaradi sinergističnega učinka obeh zdravil, in je povzročil zmanjšanje smrtnosti pitovnih piščancev.

Ključne besede: amoksicilin; alicin; učinkovitost; brojlerji; biokemjski parametri; hematološki parametri

SLOVENIAN VETERINARY RESEARCH SLOVENSKI VETERINARSKI ZBORNIK

Slov Vet Res 2020; 57 (2)

Original Research Articles

Skoczylas B, Brudnicki W, Kirkiłło-Stacewicz K, Nowicki W, Wach J. Cortical branches of the middle cerebral artery in European badger (<i>Meles meles</i>)	49
Tozon N, Biasizzo M, Ščuka L, Potočnik T, Redek M, Prem L. Reducing the number of bacterial colonies using Ecocid® S (potassium peroxy sulphate based disinfectant) at small animal clinic	55
Siddique AB, Rahman SU, Ulhaq M, Naveed R. Occurrence, molecular identification and antibiotic resistance profiling of <i>Mycoplasma gallisepticum</i> and <i>Mycoplasma synoviae</i> from chronic respiratory disease cases in poultry birds and farm environment	61
Sacha M, Weisbach N, Pöhler AS, Demmerle N, Haltner E. Comparisons of the histological morphology and in vitro percutaneous absorption of caffeine in shed snake skin and human skin	71
Aboubakr M, Elkomy A, Belih S, Morad M, Shaheen H, Abdel-Daim MM. Efficacy of amoxicillin (Atcomox®) and/or allixin on performance, haematological, biochemical, and histopathological changes in <i>Clostridium perfringens</i> infected chickens	83